

**CHARACTERISATION AND OPTIMISATION OF SOL-GEL-  
DERIVED THIN FILMS FOR USE IN OPTICAL SENSING**

by

**FIDELMA SHERIDAN, B.Sc.**

Submitted for the Degree of

**MASTER OF SCIENCE**

Presented to

**DUBLIN CITY UNIVERSITY**

Research Supervisor

**DR. COLETTE MCDONAGH,  
School of Physical Sciences,  
Dublin City University.**

**SEPTEMBER 1995**

## **Abstract.**

Both tetraethylorthosilicate (TEOS) and Liquicoat-derived sol-gel films were fabricated by dip-coating onto silicon and glass substrates. For TEOS-derived films, film thickness and temporal stability were monitored as a function of dip-speed, water:precursor ratio, sol aging time and time after dipping. Refractive indices of films were also studied. Film thickness was found to increase with sol aging time and with water:precursor ratio. The time to achieve thickness stability was decreased at higher water:precursor ratios. Film behaviour was interpreted in terms of the dependence of hydrolysis and condensation rates on the interplay between sol pH and water : precursor ratio. For Liquicoat films, refractive index and thickness as a function of time were investigated and compared with TEOS films. Refractive index tailoring was demonstrated using silica / titania Liquicoat mixtures. All films were doped with the oxygen-sensitive ruthenium complex, [Ru(II) - tris(4,7 - diphenyl - 1,10 - phenanthroline)], and optical quenching behaviour was investigated. Surface quality of all films was correlated with processing conditions. The study was motivated by the need to optimise methods and fabrication conditions for optical oxygen sensing.

## **DEDICATION**

To my mother Doreen for all of her love, support and inspiration. To Ted and the rest of the family, thanks for sticking with me.

## **ACKNOWLEDGMENTS**

I would like to thank Colette for giving me the opportunity to do this research Masters, and for her guidance and encouragement throughout. Wise words of the west from Brian, thanks! I'm especially grateful to Aisling for her companionship and support along the way, also to Ger, Thomas, Tom, Vincent, Simon, James, Fergal, Fergus, John. For the banter thanks to Kate, Siobhan, Shane, Eilish, Enda.....!

Thanks to Brian Lawless for his valuable instruction with regard to vacuums and rainbows, to Marian, Bridie, Des, John Lynch .....!

I hereby certify that this material, which I now submit for assessment on the programme of study leading to the award of M.Sc. in Applied Physics is entirely my own work and has not been taken from the work of others save and to the extent that such work has been cited and acknowledged within the text of my work.

Signed: Helena Sheridan Date: 26/9/95  
Candidate

# Table of Contents

## **Chapter 1 Introduction to Sol-Gel Thin Films and Optical Sensing**

1.1. Introduction	1
1.2. Sol-Gel Technology	1
1.3. Fluorescence and optical oxygen sensing	2
1.4. Motivation	2
1.5. Objectives of the project	3
References	4

## **Chapter 2 The Sol-Gel Process and Thin Film Fabrication**

2.1. Introduction	6
2.2. Sol-Gel Processing	6
2.2.1 The Sol-Gel Process	6
2.2.2 Hydrolysis and Condensation	8
2.3. Sol-Gel Processing Parameters	8
2.3.1 water:TEOS ratio (R)	10
2.3.2 Sol pH	10
2.3.3 Ageing Time	11
2.3.4 Catalyst type	11
2.4. Thin Film Fabrication	12
2.4.1 Principles of Dip Coating	12
2.5. Summary	14
References	14

## **Chapter 3 Fluorescence of Ruthenium Complexes and Quenching by Oxygen**

3.1. Fluorescence	15
3.2. Ruthenium Complexes	16
3.3. Quenching by Oxygen	19

3.4. Summary	20
References	20
<b>Chapter 4 Experimental Techniques</b>	
4.1 Introduction	21
4.2 Film Fabrication	21
4.2.1. Sol preparation	21
4.2.2 Liguicoat films	21
4.2.3 Substrate preparation	22
4.2.4 Coating apparatus	22
4.2.5 Film fabrication parameters	22
4.3 Film Thickness Measurement	24
4.3.1. Ellipsometry	24
4.3.2. Interferometric Microscopy	26
4.3.3. Surface Quality	28
4.4 Optical Quenching Measurement	28
4.5 Summary	30
References	30
<b>Chapter 5 Acid-Catalysed Films</b>	
5.1. Introduction	32
5.2 HCl-Catalysed (pH=1) Films	32
5.2.1. The influence of the R value on film properties	32
5.2.2. Influence of ageing time on film properties	33
5.2.3. Temporal behaviour of the films	34
5.2.4. Influence of the dipping speed on film properties	38
5.2.5. Summary	39
5.3 Catalyst	40

5.3.1. HCl films fabricated at sol pH=0.1 and pH=3	40
5.3.2 Temporal stability	41
5.4 HF-Catalysed Films	42
5.5 Summary	43
References	44
<b>Chapter 6 Liquicoat derived Thin Films</b>	
6.1. Introduction	45
6.2. Silica liquicoat films	45
6.2.1. Dip speed versus thickness and refractive index	45
6.2.2. Temporal stability	45
6.3. Silica/Titania Liquicoat Films	48
6.3.1. The influence of dip speed on thickness	48
6.3.2. Refractive Index behaviour	49
6.3.3 Thickness behaviour	49
6.4. Surface Quality	50
6.5. Summary	51
References	51
<b>Chapter 7 Quenching Behaviour</b>	
7.1. Introduction	52
7.2. Fluorescence Quenching	52
7.3. Acid Catalysed Films	52
7.4. Liquicoat Films	55
7.4.1 SiO <sub>2</sub> liquicoat films	56
7.4.2 SiO <sub>2</sub> /TiO <sub>2</sub>	58
7.5 Intensity Fall-off	59
7.6 Summary	59
References	60

## **Chapter 8 Concluding Remarks**

8.1 Overall Summary and Conclusions	61
8.2 Optimisation of film for oxygen sensing	61
8.3 Achievement of objectives	62
8.4 Refereed Publications arising from this project	62

# **Chapter 1 Introduction to Sol-Gel thin films and Optical sensing**

## **1.1 Introduction**

The project deals with sol-gel-derived films doped with a ruthenium complex whose fluorescence is quenched in the presence of oxygen. This chapter aims to introduce the above topics. A brief account will be given of the sol-gel process, fluorescence and optical sensing. These topics will be dealt with in more detail in subsequent chapters. Finally the overall background and motivation of the project will be discussed.

## **1.2 Sol-gel technology**

Sol-gel processing involves hydrolysis and condensation of organic precursors at relatively low temperatures to form porous glass. Glasses can be made with specific properties by manipulation of the initial processing parameters[1]. Using different precursors a variety of glass can be prepared. Since the initial sol containing the precursor is liquid, production of thin films by various coating processes as well as monoliths is possible. As a result of this there are many products which are sol-gel derived including anti-reflection coatings, protective films and monolithic glass. Sol-gels can be used as catalyst supports, as laser and non-linear optical materials[2,3,4] and for sensor applications[5,6,7,8]. In this project, the sol-gel film is used as a support for an oxygen sensitive fluorescent complex.

### **1.3 Fluorescence and optical oxygen sensing**

Fluorescence occurs when an excited electron decays radiatively, i.e. with the emission of a photon of light. Fluorescent materials are becoming increasingly important in optoelectronics, for example in the area of lasers, non-linear optics and optical sensing[9,10]. The determination of oxygen concentration is based on collisional quenching by molecular oxygen of a fluorophore embedded in a support matrix, in this case a sol-gel film. Currently available oxygen sensors are based on electrochemical and amperometric principles, for example, the Clark Electrode[11]. Optical oxygen sensors are more attractive because they are not easily poisoned, they offer the possibility of miniaturisation, they do not consume oxygen and have a fast response time. Developments in optical oxygen sensing have been facilitated by the availability of new LED sources and photodiode detectors[12,13]. Optical-fibre-based sensors offer the possibility of remote and distributed sensing[14] in hostile environments. In this laboratory, gas phase and aqueous phase optical oxygen sensors have been developed which are based on fluorescence-intensity quenching of the ruthenium complex (Ru -tris (4,7-diphenyl-1,10-phenanthroline)), which has been entrapped in a porous sol-gel-derived film [15].

### **1.4 Motivation**

This project was motivated by the need to optimise sol-gel films for optical oxygen sensing. Commercially viable sensors require films which are robust with long-term stability and reproducible quenching behaviour. One of the distinctive features of the sol-gel process is that film properties can be tailored by adjusting various processing parameters (see Chapter 2). In this work film properties were monitored as a function of a number of different processing parameters, for example water:precursor ratio, sol pH, type of catalyst and curing time and temperature. Film properties monitored

include thickness, refractive index, fluorescence quenching behaviour and surface quality.

## **1.5 Objectives of the project**

The principle objectives were:

- To investigate film properties as a function of water:precursor ratio in the sol.
- To investigate the influence of sol ageing time.
- To investigate the influence of different catalysts.
- To compare films synthesized in the laboratory with commercial "Liquicoat" films.
- To identify optimum film processing parameters for oxygen sensing.

## **References:**

- [1] Brinker, C.J., Scherer, G.W. **"Sol-Gel Science"** Academic Press, (1990)
- [2] Sakka, S., **"The Current State of Sol-Gel Technology"** Journal of Sol-Gel Science and Technology, 3,369-81 (1994).
- [3] Buckley, A.M. and Greenblatt, M., **"The Sol-Gel Preparation of Silica Gels"** Journal of Chemical Education volume 71, Number 7, page 559, (1994).
- [4] Ganguli, D., **"Sol-Gel Processing of materials for electronic and related applications"** Bull. Material Science, Volume 15, Number 5, pp 421-430, (1992).
- [5] MacCraith, B.D., O'Keeffe, G., McEvoy, A., McDonagh, C., McGilp, J.F., O'Kelly, B., O'Mahony, J., Cavanagh, M. **"Light-emitting-diode-based oxygen**

- sensing using evanescent wave excitation of a dye-doped sol-gel coating**", Opt. Engin. Vol. 33, 12, pp3861-3866, (1994).
- [6] Avnir, D., Braun, S., Lev, O., Levy, O., Ottolenghi, M., "**Chemically active organically doped sol-gel materials: Enzymatic sensors, chemical sensors and photoactive materials**", SPIE Vol. 1758 Sol-Gel Optics II (1992).
- [7] Bacon and Demas, J.N., "**Determination of Oxygen Concentration by Luminescence Quenching of a polymer-immobilised Transition-Metal Complex**" Analytical Chemistry, Volume 59, Number 23, (1987).
- [8] Demas, J.N. and DeGraff, B., "**Design and Applications of Highly Luminescent Transition Metal Complexes**" Analytical Chemistry, Volume 63, Number 17,(1991).
- [9] Lippitsch, M.E. and Droxler, S., "**Luminescence decay-time-based optical sensors: principles and problems**" Sensors and Actuators B, 11, pp97-101, (1993)
- [10] Wolfbeis, O., "**Fibre Optical Fluorosensors in Analytical and Clinical Chemistry**" Luminescence Spectroscopy: Methods and Applications-Part II; edited by Stephen J. Schulman., Wiley and Sons, Inc., (1988).
- [11] Clark, L.C., Journal of Transactions- American Society for Artificial Internal Organisation, Volume 2, p41, (1856).
- [12] MacCraith, B.D., O'Keefe, G., McEvoy, A., McDonagh, C. "**Development of a LED-based fibre optic oxygen sensor using a sol-gel-derived coating**", Chemical, Biochemical and Environmental Fibre Sensors 6, San Diego, SPIE Vol. 2293, pp. 110-120. (1994).
- [13] MacCraith B., Ruddy V., Potter C., "**Optical waveguide sensor using evanescent excitation of a fluorescent dye in a sol-gel glass**". Electronics Letters, Volume 14, Number 27 pp1247-1248, (1994).

- [14] Lieberman R.A., Blyler L., Cohen L., "A **distributed fibre optic sensor based on cladding fluorescence**" Journal of Lightwave Technology, Volume 8, Number 2, (1990).
- [15] McEvoy, A., McDonagh, C.M., MacCraith, B.D., "Development of a fibre optic dissolved oxygen sensor based on quenching of a ruthenium complex entrapped in a porous sol-gel film", Journal of Sol-Gel Science and Technology, accepted for publication, (1995).

## **Chapter 2 The Sol-Gel Process and Thin Film Fabrication**

### **2.1 Introduction**

This section details the reactions involved in sol-gel processing. The variety of parameters within the process will be considered in terms of their influence on the resulting thin films. A number of coating processes will be introduced and the dip coating process will be discussed in detail.

### **2.2 Sol-gel processing**

Sol-gel processing enables the production of porous homogenous glass at ambient temperatures. It involves the hydrolysis and condensation of an alkoxide precursor in the presence of water, a catalyst and solvent. For silica glasses a silicon alkoxide is used as a precursor, the most commonly used being tetraethylorthosilicate,  $\text{Si}(\text{OC}_2\text{H}_5)_4$  known as TEOS.

#### **2.2.1 The Sol-Gel Process**

The first step in the process is the mixing of the alkoxide precursor with water in the presence of a mutual solvent (e.g. ethanol) and a catalyst (which can be acidic or basic) [1]. After mixing the sol is left to age, (i.e. the reactions of hydrolysis and condensation are left to proceed for a time known as the ageing time), until such time that the sol is viscous enough for further processing. If left for long enough the sol will gel at a time known as the gel point, this point being determined by the initial processing parameters. Ageing can be carried out in elevated temperatures if required. A schematic of the process is illustrated in figure 2.1.

For the production of thin films the sol is coated onto a substrate after a given ageing time. Coating generally is done by spin coating or dip coating. After coating the film can be densified as needed by drying in an oven or at room temperature.

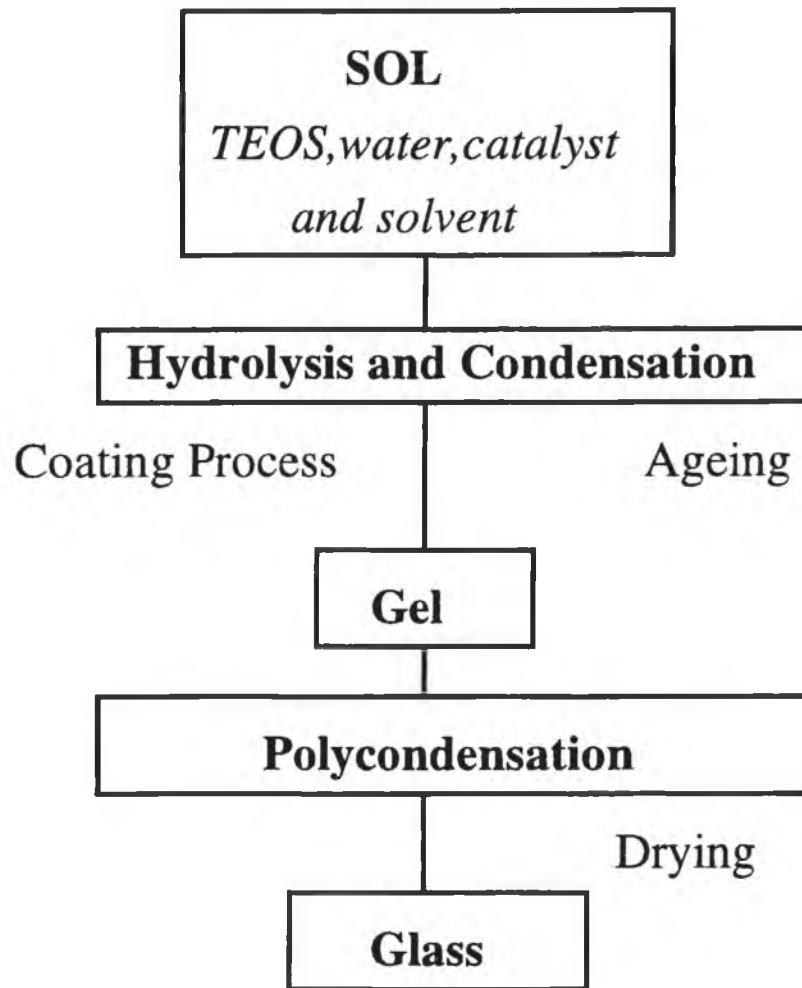


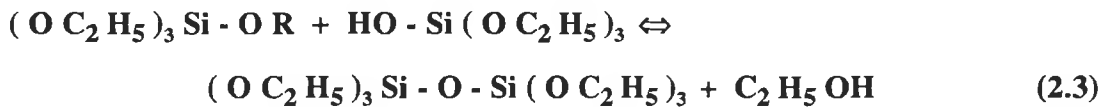
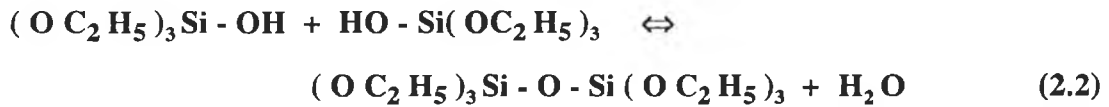
**Figure 2.1** The Sol-Gel Process

### 2.2.2 Hydrolysis and condensation:

For silica glass TEOS is hydrolysed when in the presence of water. The hydrolysis reaction replaces alkoxide with hydroxyl groups as shown in equation 1 and Figure 2.2, [1].



The condensation reactions, shown in equation 2.2 and 2.3, yield by-products of alcohol and water. They generally begin before hydrolysis is complete. It is these processes which build up a three dimensional Si-O-Si network.

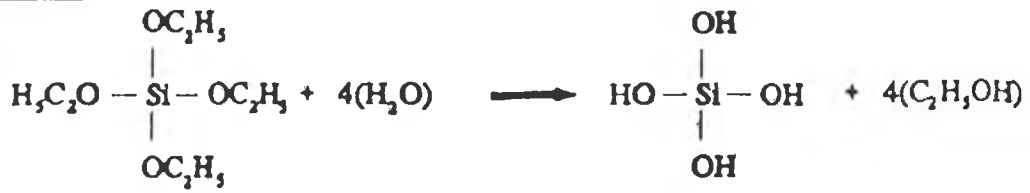


Material properties are influenced by parameters such as sol pH and water:TEOS ratio as discussed in the next section.

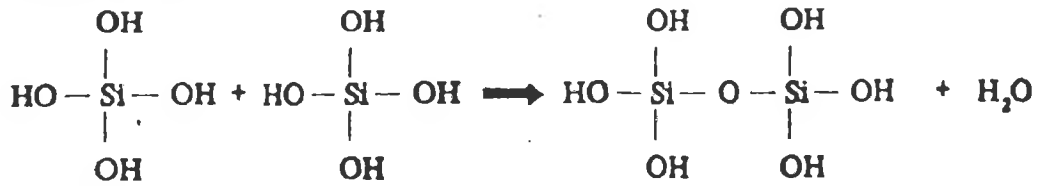
## 2.3 Sol-Gel Processing Parameters

The processing parameters of relevance to this work are the molar ratio of water to precursor, hereafter referred to as R, the sol pH, ageing or prepolymerisation time and catalyst type. Other parameters which are not varied in this investigation but

Hydrolysis



Condensation



Polycondensation

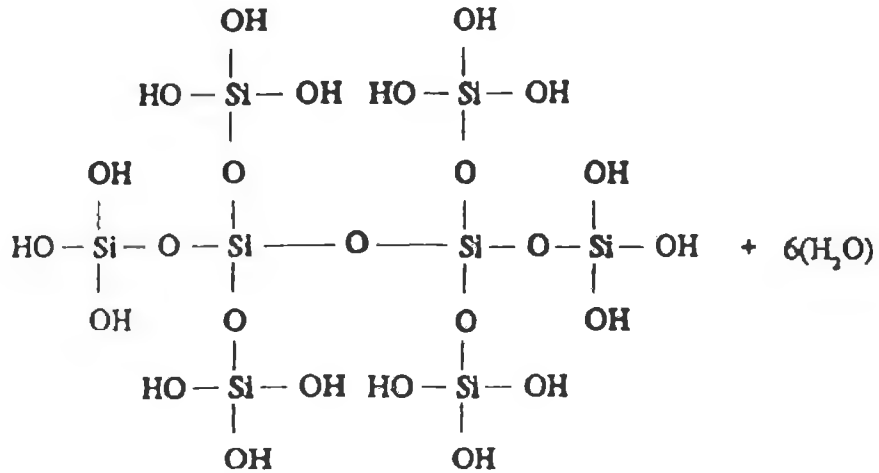
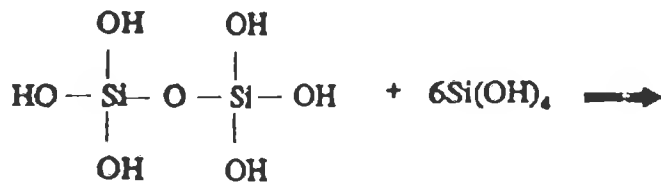


Figure 2.2 Schematic of hydrolysis and condensation reactions

which influence the final structure include solvent type, precursor type, curing temperature[1]. A brief discussion of the relevant parameters is now given.

### **2.3.1 Water:TEOS ratio (R):**

The molar ratio of water to TEOS influences the structural evolution of sol-gel materials because of the role of water in the hydrolysis and condensation processes. The stoichiometric water:TEOS ratio (R) for complete hydrolysis is  $R=2$ . However, due to the formation of intermediate species and reverse reactions  $R=2$  is not sufficient for complete hydrolysis [1,2]. With an increase in the amount of water present there is an increase in the relative rates of hydrolysis and condensation with respect to rates for lower R values, at a given pH value, which decreases the gel time of a sol. Thus as R increases the sol will become more viscous and will produce a thicker film. However there is an optimum amount of water beyond which the excess of water serves to dilute the sol and decreases film thickness as discussed in chapter 5.

### **2.3.2 Sol pH:**

The pH of the starting solution influences the relative rates of hydrolysis and condensation. pH 2 is the isoelectric point of silica, at which point the electron mobility and surface charge is zero.[1]. This pH value acts as a boundary between so-called acid catalysis of the polymerisation process ( $\text{pH} < 2$ ) and base catalysis ( $\text{pH} > 2$ )[1]. Acid catalysis is associated with rapid hydrolysis and relatively long gel times. Basic catalysis involves much faster condensation rates, slower hydrolysis and shorter gel time. The behaviour of condensation as a function of pH is shown in figure 2.3. In the limit of low pH( $<2$ ) and low R ( $<2$ ), the gel evolves as a weakly-branched microporous structure with pore sizes  $< 2\text{nm}$ . Under conditions of  $\text{pH}>2$  and  $R>2$  a particulate gel is formed with larger pores [1].

### 2.3.3 Ageing Time:

The time between mixing of the precursor, water, catalyst and solvent and the time for coating is known as the ageing time. It is the period where hydrolysis and condensation are allowed to proceed in ambient surroundings or in elevated temperatures. The sol becomes more viscous during ageing due to the cross linking inherent in the condensation reaction, yielding thicker films.

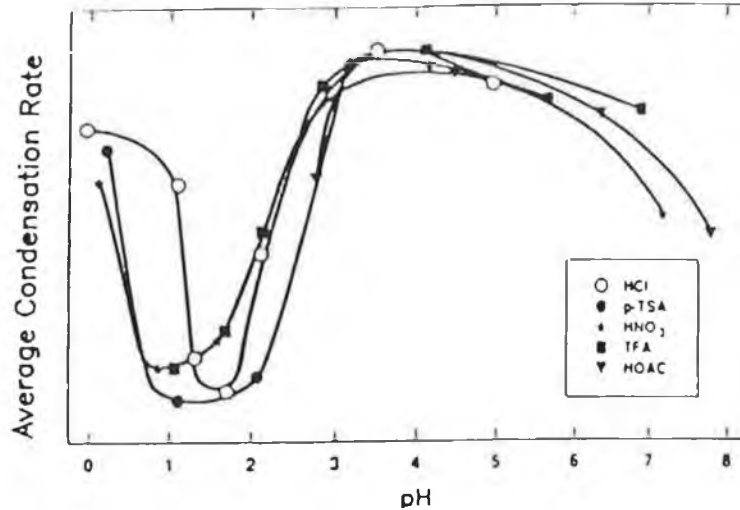


Figure 2.3 Condensation rate as a function of pH [2]

### 2.3.4 Catalyst Type:

Hydrolysis and condensation rates are enhanced via addition of acids or bases. Acids protonate negatively charged alkoxide ligands. The silicon becomes more hydrophilic and thus more easily hydrolysed[1]. Under basic conditions, water dissociates to give hydroxyl anions which attack the silicon atoms. It is known that different acids effect the processes to different extents due to the role played by the anion [1,3]. For example when HF is used as a catalyst, F<sup>-</sup>, being about the same size as OH<sup>-</sup>, catalyses both hydrolysis and condensation. Hence HF catalysed sols behave similarly to base catalysed sols, gelation times decrease and porosity and pore size are increased.[3]

## 2.4 Thin Film Fabrication

Spin-coating and dip-coating are the two most commonly used coating techniques for thin film production. Spin coating requires a small amount of solution for coating, so there is little waste. It does not work well for substrates that are large, or for substrates that are not circular[4]. Dip coating is suitable for use for any shape or size of a substrate. Apparatus is relatively simple and inexpensive. A large volume of solution is required compared to spin coating and both sides of the substrate are covered. Dip coating was the method chosen for this work as it enables coating of both planar and optical fibre substrates. In this laboratory, characterisation of the thin films is carried out mainly on planar glass and silicon slides. Optical fibres are coated for some specific sensor applications not dealt with here.

### 2.4.1 Principles of Dip Coating

Generally during dip coating a substrate is immersed in a solution and then drawn out at a constant velocity. In our laboratory the sample is held rigid and the solution is held on a moving stage and is drawn away from the sample. After coating, the sample is left to reach equilibrium; flow from top to bottom of the substrate continues. As long as there is no disturbance in the dipping environment such (as vibration or air movements) an even film should form down to the bottom of the slide, where there will be a small uneven deposit of sol. From this point on the film is constrained in the plane of the substrate and any subsequent shrinkage will occur in the plane normal to this. This is observed as a gradual reduction of the film thickness. The relationship between film thickness ( $t$ ) and dipping speed ( $S$ ) for Newtonian fluids is

$$t = 0.95 (N_{ca})^{1/6} (\eta S / \rho g)^{1/2} \quad (2.4)$$

where  $\eta$  is viscosity,  $\rho$  is the density,  $g$  is the acceleration due to gravity,  $Nca$  is equal to  $\eta S/d$ ;  $d$ =surface tension[5]. Other parameters in the coating process which influence film properties are:

**(1) Substrate cleanliness**

It is very important that substrate surfaces are clean and contamination free for the duration of processing. Surfaces should also be homogenous in quality and preferably polished. Variations arising from either of the above will interfere with the coating process and will give rise to non-uniformity and flaws in the resulting film[4].

**(2) Coating liquid contamination**

High purity reagents and solvents must be used in the preparation of the sol. However there is always risk of contamination from the environment or from deterioration of solutions. In these cases sometimes filtration can be used to produce the desired purity.

**(3) Coating environment**

In order to achieve high quality films it is necessary to coat substrates in a vibration- and draught-free environment. Vibration absorption apparatus and a perspex covering of the working apparatus will generally suffice. Slides should be protected until drying is complete.

**(4) Drying**

After dipping, the thin films are put in an oven at a known temperature for an extended period known as the drying time. The films are held much as they are during dipping, i.e. at the top with all sides exposed to the air. Drying serves to drive off excess fluids and densify the film[1].

## 2.5 Summary

The main features of the sol-gel process have been discussed and its flexibility illustrated. Thin film fabrication has been introduced with emphasis on the dip-coating method which was chosen for film deposition in this work.

### References:

- [1] Brinker, C. J. and Scherer, G.W. "**Sol-Gel Science**" Academic Press, (1990).
- [2] Coltrain, B.K. et al., Proceedings of the IV Int'l. Conference on Ultrastructure Processing of Ceramics, Glasses and Composites, Wiley, (1989)
- [3] Pope, E.J. and Mackenzie, J.D. "**Sol-Gel Processing of Silica - II The role of the catalyst**" Journal of Non-Crystalline Solids 87,pp185-198, (1986)
- [4] Thomas, I.M. "**Optical Coating Fabrication**" Sol-Gel Optics, Processing and Applications, edited by L.C.Klein. The Kluwer International Series in Engineering and Computer Science.
- [5] Strawbridge, I. and James, P.F., "**The factors affecting the thickness of sol-gel derived silica coatings prepared by dipping**", Journal of Non-Crystalline Solids, Vol. 86, pp381, (1986)

## Chapter 3 Fluorescence of Ruthenium Complexes and Quenching by Oxygen

### 3.1 Fluorescence

Fluorescence is the emission of non-thermal electromagnetic radiation from a molecule as it makes the transition from an excited state to a lower state. The emitted photons have an energy equivalent to the energy difference between the two levels involved. In order to populate the excited states an energy source (e.g. photon source, energy from electron collisions or from chemical reactions) is necessary. Figure 3.1 illustrates the basic excitation and emission processes. Transitions occur between all of the electronic levels. However, not all de-excitation processes result in the emission of visible radiation. Generally electrons are excited by incident photons to the upper level E(2). Through radiative and non-radiative (e.g. thermal phonons) emissions the absorbed energy is released and electrons return to ground level. Non-radiative decay occurs if the energy level gaps are small (e.g E(2) to E(1)). For the fluorescent complex in this work radiative decay arises from the triplet state. A triplet state occurs where the electron in the excited state has the same spin as the electron in the lower state. Pairing of electrons where the spins are opposite gives rise to singlet excited states.[1] Fluorescent lifetime ( $\tau$ ) is the time spent in the excited state prior to fluorescence. When radiative decay occurs between two singlet states, the transition is quantum mechanically allowed and lifetimes are of the order of 10ns. Emission also occurs when a triplet state excited electron returns to a singlet ground state. These transitions are quantum mechanically forbidden and lifetimes are longer[1]. Where decay results in radiation the emitted photons have energies

$$h\nu_1 = E(1) - E(0) \quad (3.1)$$

where  $\nu$  = the frequency of the fluorescent emission,  $h$  = Planck's constant.

Photons emitted by fluorescence always have less energy and greater wavelength than those absorbed due to the various non-radiative energy losses[2]. This shift in wavelength is beneficial as it reduces the need for filtering devices for fluorescence detection [3].

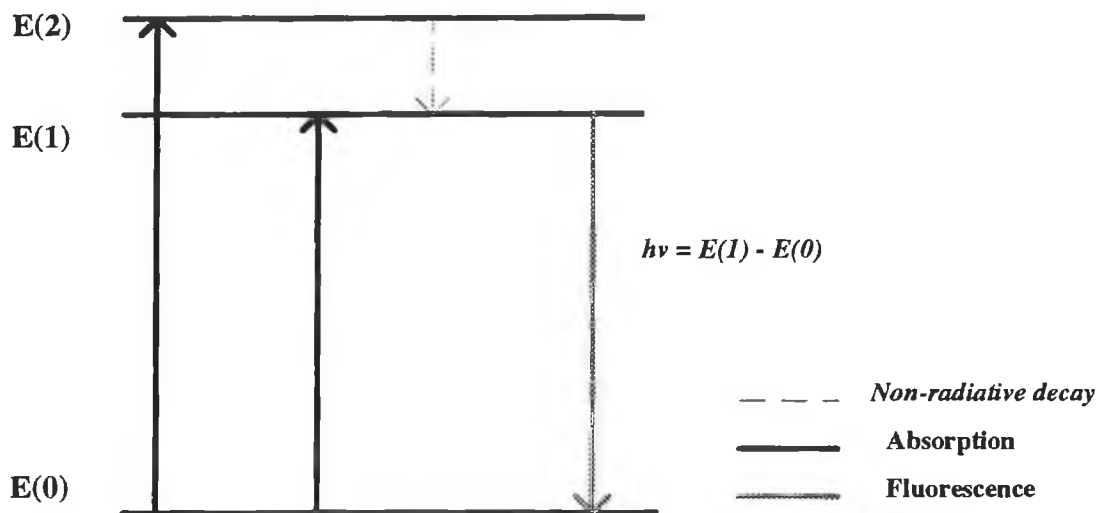
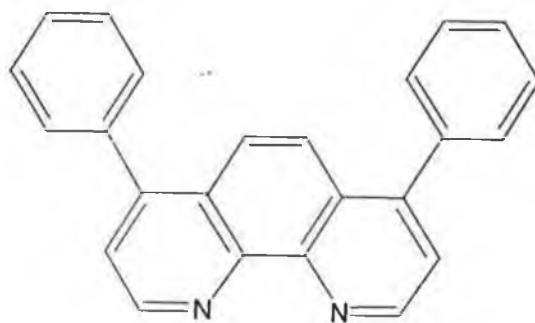


**Figure 3.1 Basic Excitation and Emission Processes**

### 3.2 Ruthenium Complexes

Transition metal complexes are highly fluorescent and are widely used in optical sensor applications[3]. They generally have high quantum yields (ratio of the number of photons emitted to those absorbed), and long life-times ( $>5\mu\text{s}$ ). Absorption bands generally occur in the UV/blue region of the spectrum, while emission is at wavelengths of approximately 600nm, compatible with photo-detectors. With this large shift between absorption and emission, excitation and detection signals for sensor applications are easily distinguished. Transition metals are also stable

thermally, chemically and photochemically. Of the transition metals, ruthenium is one of the more widely used in sensor technology. In this work the ruthenium complex Ru(II) tris(4,7-diphenyl-1, 10-phenanthroline) or  $[\text{Ru}(\text{Ph}_2\text{phen})_3]^{++}$  is chosen as an oxygen sensitive compound that is incorporated into the sol-gel film. Figure 3.2 illustrates the chemical structure of the ligand ( $\text{Ph}_2\text{phen}$ ) which attaches itself to the ruthenium molecule via nitrogen atoms (N), each ruthenium molecule has three of these ligands surrounding it. Figure 3.3 shows the schematic energy levels.  $\Phi_{\text{ISC}}$  is a non-radiative transition between triplet and singlet states, MC is a metal centered state, and  $k_r+k_{nr}$  is the sum of the radiative and non-radiative decay constants. The main absorption band is at 460nm, corresponding to absorption from the ground state (GS) to the upper singlet state[3]. The emitting state is a metal to ligand charge transfer (MCLT) state, arising from ruthenium metal electron transferred to a ligand orbital. The emission is centered at 610nm as shown in figure 3.4.



4,7-diphenyl,1,10-phenanthroline ( $\text{Ph}_2\text{phen}$ )

**Figure 3.2** Chemical structure of Ru(II) tris(4,7-diphenyl-1, 10-phenanthroline)

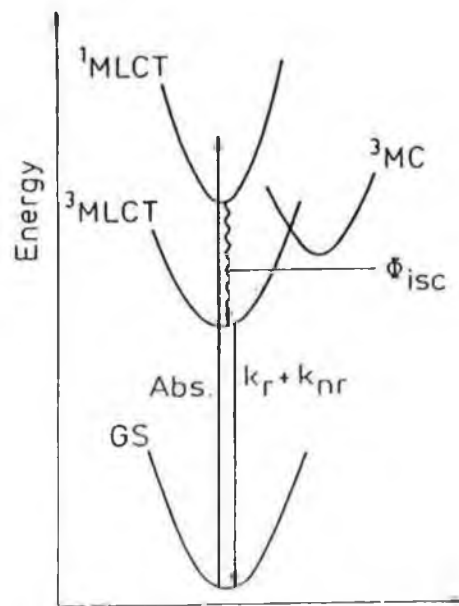


Figure 3.3 Schematic of energy levels of a ruthenium complex

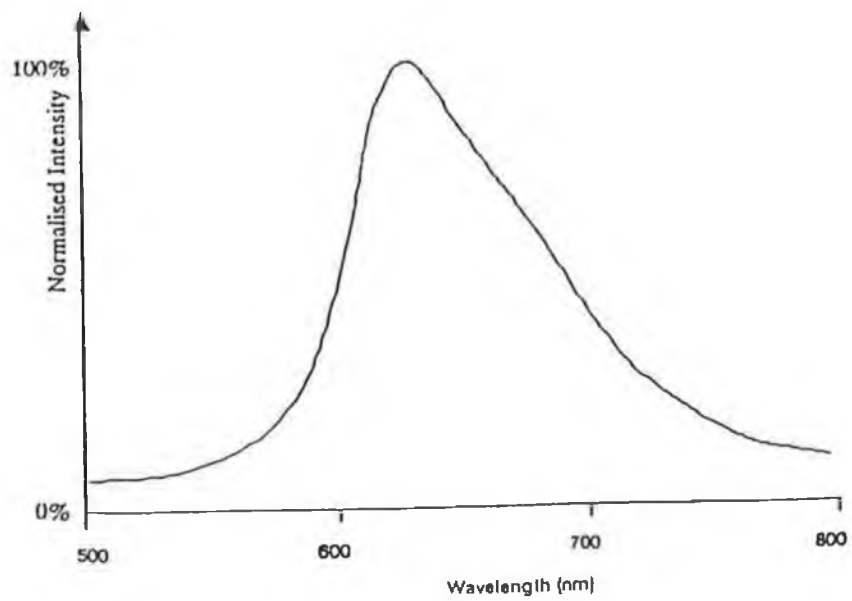


Figure 3.4 The fluorescence spectrum of the ruthenium complex

### 3.3 Quenching by Oxygen

Fluorescence quenching is any process which depopulates the excited state without emission of a photon. There are two forms of quenching: *static* which occurs due to the formation of a non-fluorescent ground state complex between fluorophore and quencher, and *dynamic* where quenching is a result of collisional encounters between the quencher and the fluorophore. In this work dynamic quenching occurs. When an oxygen molecule collides with the complex in the excited state, an oxyciplex forms, which returns to the ground state. The oxygen dissociates and therefore is not consumed in the process. Quenching is proportional to the concentration of the quencher and its ability to diffuse to the fluorophore in a time less than that of the excited state lifetime. It affects both the intensity and the lifetime of the fluorophore, both decreasing as quencher concentration increases. The Stern Volmer equation describes the process by relating the quencher concentration to the extent of quenching

$$I_0/I = 1 + K_{SV}(Q) \quad 3.2$$

$$K_{SV} = k \tau_0 \quad 3.3$$

where  $I_0$  and  $I$  are the fluorescence intensities in the absence and presence of quencher, respectively,  $K_{SV}$  is the Stern-Volmer quenching constant,  $Q$  is the quencher concentration,  $k$  is the bimolecular quenching coefficient and  $\tau_0$  is the excited state lifetime [4]. In the simplest case of single exponential fluorescence decay in the presence of oxygen, (equation 3.2), a plot of  $I_0/I$  versus oxygen concentration

should yield a straight line of slope  $K_{SV}$  and intercept at  $y=1$ .  $K_{SV}$  is directly proportional to  $D$  the diffusivity of the gas through the film.

### **3.4 Summary**

This chapter introduced the fundamental principles of fluorescence and fluorescence quenching. The use of transition metals in sensing was outlined, with emphasis on that of  $[\text{Ru}(\text{Ph}_2\text{phen})_3]^{++}$  which was used in this work.

### **References:**

- [1] Lakowicz J., "**Principles of Fluorescence Spectroscopy**", Plenum Press, (1983).
- [2] Gilbert, A., and Baggot, J.E., "**Essentials of Molecular Photochemistry**", Blackwell publications.(1991).
- [3] Demas, J.N., DeGraff, B.A. "**Design and Applications of Highly Luminescent Transition Metal Complexes**", Analytical Chemistry Vol.63 No.17, (1991).
- [4] Stern, O., Volmer, M., M. Phys.Z. Volume 20, 183, (1919)

## **Chapter 4 Experimental Technique**

### **4.1 Introduction**

This chapter details methods used in the fabrication of sols and thin films. The significance of various initial processing parameters has been dealt with in chapter 2. With reference to this, a description of how each was varied in this work is given. The chapter then discusses methods and instrumentation used in the characterisation of thin films.

### **4.2 Film Fabrication**

#### **4.2.1 Sol Preparation**

In the laboratory, sols are prepared using an alkoxide known as tetraethylorthosilicate (TEOS), ethanol and de-ionised water containing the acid catalyst. For a predoped sol the appropriate amount of ruthenium complex (20,000 parts per million) was weighed into a clean glass vial. To this was added the correct amount of ethanol and water (pH=1), and the solution was stirred. TEOS was then added to the solution dropwise to allow for the immiscibility of water and the precursor. Generally sols were left to stir for 1 hour before ageing. Prior to ageing the vial was closed tightly, and the top was pierced with a needle once to allow for some evaporation. It was then placed in an oven at a temperature of 70°C for the required ageing time.

#### **4.2.2 Liquicoat Films**

Commercial sol-gel solutions are available from E. Merck. Two kinds were purchased: Liquicoat solutions: Si ZLI-2132 and Ti ZLI-1837, which are used to produce silica and titania coatings respectively. Silica and mixed silica/titania solutions

were coated onto glass and silicon slides. For mixed silica/titania films, the required volumes of the two solutions were mixed thoroughly just before coating. For doped solutions the dopant was dispensed first, liquicoat was added and the solution was stirred vigorously. After coating, liquicoat films were dried as recommended by the manufacturer, for a minimum of 10 minutes at 100°C.

#### **4.2.3 Substrate Preparation**

Glass microscope slides and silicon wafers were cut and cleaned as follows: the substrates were first washed in de-ionised water, then in methanol and acetone and subsequently they were conditioned in de-ionised water at 70°C for 24 hours.

#### **4.2.4 Coating apparatus**

The dipping apparatus is shown in figure 4.1. It consisted of a moveable stage which was connected to a stepper motor under computer control. The sol was held in a vial on the stage and moved to immerse the slide. It was then pulled away at a constant rate. Sols of varying R values, pH and catalysts and liquicoat sols were coated onto substrates at a variety of dipping speeds between 0.5mm/s and 1.7mm/s. Sols were left to reach ambient temperatures before dipping. Substrates were cleaned as described previously. A perspex covering acted as a draught guard and vibration dampers were incorporated in the apparatus to facilitate the production of good quality films.

#### **4.2.5 Film fabrication parameters**

##### **(i) water:TEOS ratio (R)**

As referred to earlier (section 2.3.1) the water:TEOS ratio, R, greatly influences the structure of the film. Sols were made with HCl as a catalyst at pH=1, with R values of

2,4,6,7 and 8. The resulting films were subsequently characterised and compared with one another.

**(ii) pH**

Generally the pH used in the fabrication of standard HCl catalysed, R=2 slides was pH=1. In this work pH=0.1 and pH=3 were also investigated in the fabrication of otherwise standard sols. Technically, in sol-gel terms pH=3 is a base catalyst[1]. Gel times, thicknesses, temporal stability and quality of the resulting films were monitored.

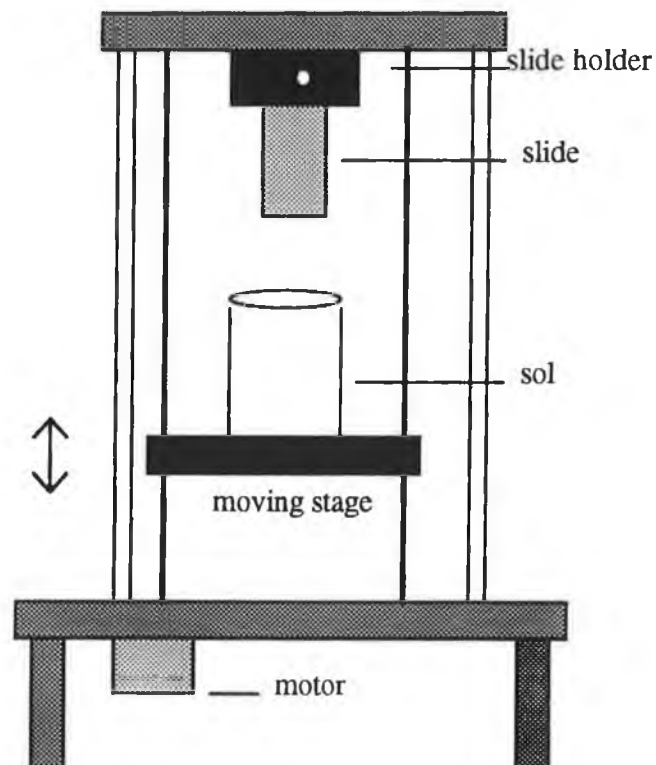


**Figure 4.1 Dip-Coating Apparatus**

### **(iii) Catalyst**

Although HCl was the catalyst most commonly used, sols of  $R=2$  and  $pH=1$  were also prepared with HF as catalyst. The resulting films and sols were compared to those of a HCl catalysed sol of  $pH=1$  and  $R=2$ . It should be noted that due to the rapid gelling time inherent in HF catalysed sols [2] the ageing programme was at room temperature for 24 hours.

### **(iv) Ageing time**

Ageing times were varied for acid (HCl) catalysed sols of  $R$  values 2, 4 and 6. Slides were dip coated after different ageing times using sols where viscosity was great enough to adhere to the substrate surface but fluid enough to coat evenly. Quality, thickness and refractive index of the resulting films were studied.

### **(v) Drying time/temperature**

After dipping the thin films were held vertically in an oven for a period known as the drying time. In order to investigate the influence of drying time on the properties of HCl catalysed,  $R=2$  samples where the sol was aged for 18 hours, slides were dried for times between 1 hour and 120 hours. The drying temperature in this experiment was  $100^{\circ}\text{C}$ . Liquicoat samples were also exposed to a drying temperature of  $100^{\circ}\text{C}$  for drying times ranging between 10 minutes (see section 4.2.2) and 120 minutes. The results in terms of initial thickness and temporal stability of each were investigated.

## **4.3 Film Thickness**

### **4.3.1 Ellipsometry**

Ellipsometry was used to measure the initial thickness, refractive index, and the thickness stability over time. This apparatus was chosen as it is much more sensitive than other techniques such as interferometry[3]. It can determine refractive indices of

films of unknown thicknesses. The ellipsometer used was a Rudolph Research Auto-El III. In ellipsometry a monochromatic, polarised beam is incident on a film at an angle of incidence, in this case  $70^\circ$ . On traveling through the sample film to the substrate it is reflected at an angle equal to the angle of incidence. Due to passage through the sample layer the polarisation of the beam changes. In measuring that change software in the system relates it to the thickness and refractive index of the film.

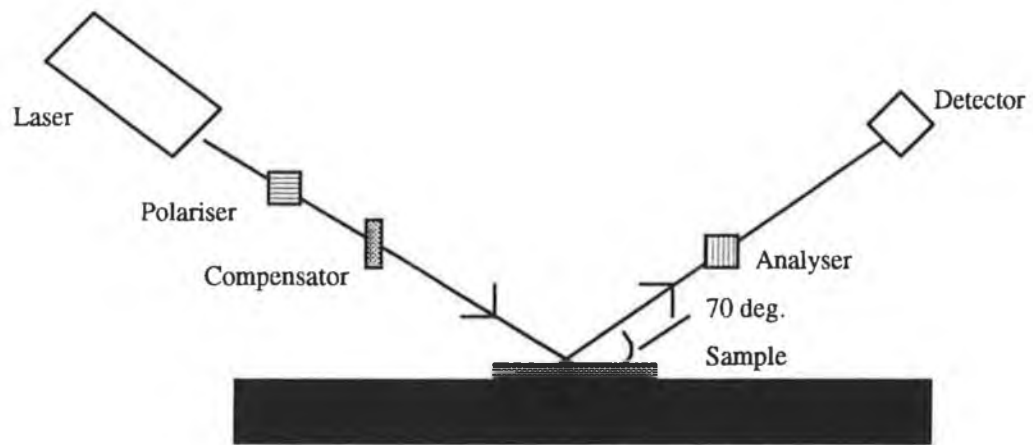


**Figure 4.2 Schematic of Ellipsometry**

The ellipsometer is composed of a laser, polariser, analyser, compensator and detector. Generally the compensator is held at a fixed angle about the optical axis with respect to the plane of incidence (the film) and biases the system to the region of most response to the changing parameter. Measurement involves setting the incident (and thus the reflected) beam axis at an angle of  $70^\circ$  relative to the sample. The

polariser and analyser are rotated alternately until the intensity of the beam incident on the detector is at a minimum. At this point the angles of the polariser and analyser are measured and are converted to parameters known as  $\Delta$  and  $\Psi$ .  $\Delta$  and  $\Psi$  are functions of the incident angle, the wavelength of light, the refractive index of the ambient medium as well as the real and imaginary refractive indices of the substrate and the sample thickness and refractive index. Given that some of these are known, the software incorporated within the ellipsometer uses these parameters to determine film thickness and refractive index. When the optical path length of the light traversing the film reaches an integer number of wavelengths,  $\Delta$  and  $\Psi$  are the same as for no film at all. The ellipsometer gives readings of the full cycle thickness  $S$ , the zero order thickness  $T$  and the refractive index of the thin film[4]. Thus the actual thickness of the film might be  $T$ ,  $T+(S)$ ,  $T+2(S)$ ,..... and it is necessary to have an independent measure of thickness as discussed in the next section. On average six readings were taken on the ellipsometer and the standard deviation was 20nm.

#### **4.3.2 Interferometric Microscopy**

Due to the cycle effect inherent in ellipsometry as discussed in the preceding section, an independent estimation of the thickness of a film is required. Interferometric Microscopy provides such a facility. Prior to microscopy the thin film and its substrate must be coated with a thin layer of a reflective material such as aluminum. This was carried out by vapour deposition in an Edwards Auto 306 vapour deposition chamber. The appearance of the film is outlined schematically on figure 4.3(a).

Interferometric microscopy[5] is based on two beam interferometry and is performed using a purpose-made objective for the microscope, (Nikon model 272285) which has a reflection reference in its centre. A half mirror is interposed between the objective lens and the specimen. The components are arranged so that an interference pattern appears when the system is focused on the sample. On looking at the interface

between the substrate and the film one sees that there is a shift in fringes across the boundary due to the different relative heights of the film and substrate. A schematic diagram is shown in figure 4.3(b), while a photograph of an actual fringe shift is shown in figure 4.4. This shift is measured (number of fringes) and then multiplied by half the average wavelength of white light (275nm) to yield an indication of the order of thickness.

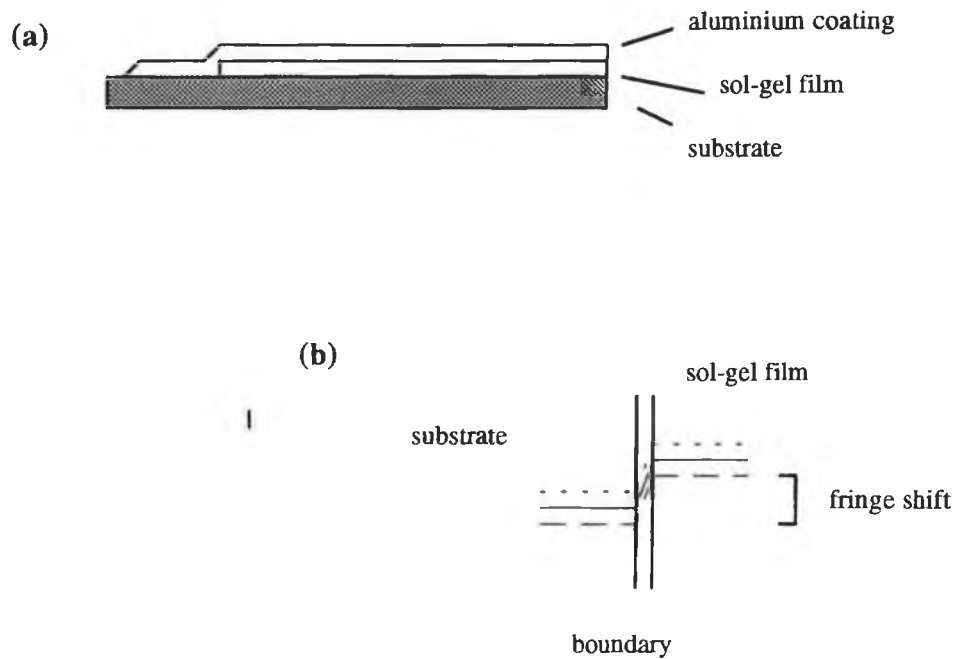


**Figure 4.3 (a) Sample prepared for Interferometric Microscopy**  
**(b) Fringe Shift Schematic**

The thickness of the film  $t(\text{nm})$ , the mean wavelength of the light source  $\lambda(\text{nm})$  and the fringe shift ( $n$ ) are related as follows:

$$t = n (\lambda / 2) \quad (4.1)$$

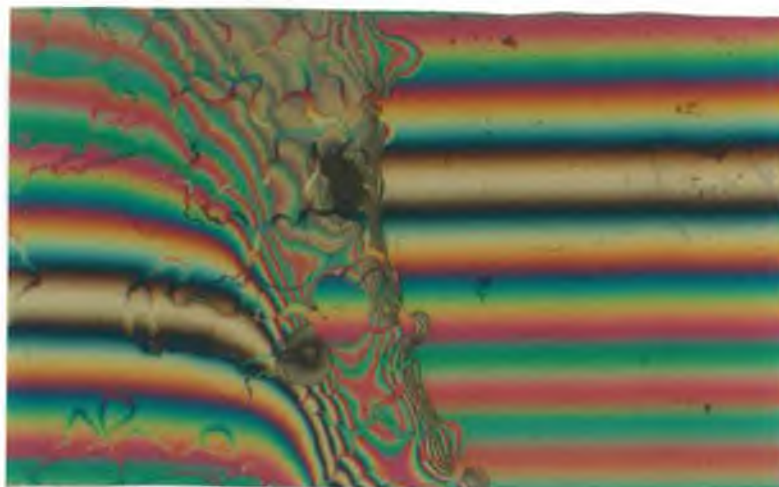


**Figure 4.4 The Fringe Shift**

#### **4.3.3 Surface Quality**

Using a Nikon microscope (model 272285) with an objective lens (20x100), the quality and homogeneity of all films were investigated. Comparisons were drawn in terms of overall quality of a film and quality of sample edges.

#### **4.4 Optical Quenching Measurement**

Doped films were characterised in terms of their sensitivity to oxygen using the apparatus shown in figure 4.5. It consisted of a Fasco Industrial Inc. Argon-ion laser (type U62B) for excitation, a Jobin Yvon 1m focal length monochromator (set at 610nm), a Hamamatsu R928 photomultiplier tube for detection, a current to voltage converter between the PMT and a Brookdeal Electronics 5206 Two Phase Lock-in-

Amplifier, a Bytronics interface card (MPIBM3A) and a P.C. for data storage and analysis. A line filter at 488nm (excitation wavelength) and a narrow band interference centered at 610nm (fluorescent wavelength) were used, as were focusing optics. The sample slide was held in a gas cell within which it was exposed to various controlled mixtures of oxygen and nitrogen. The gases were dispensed from mass flow controllers produced by Unit Instruments (UFC 1100A). A schematic of the sample chamber and gas flow arrangement is shown in figure 4.6.

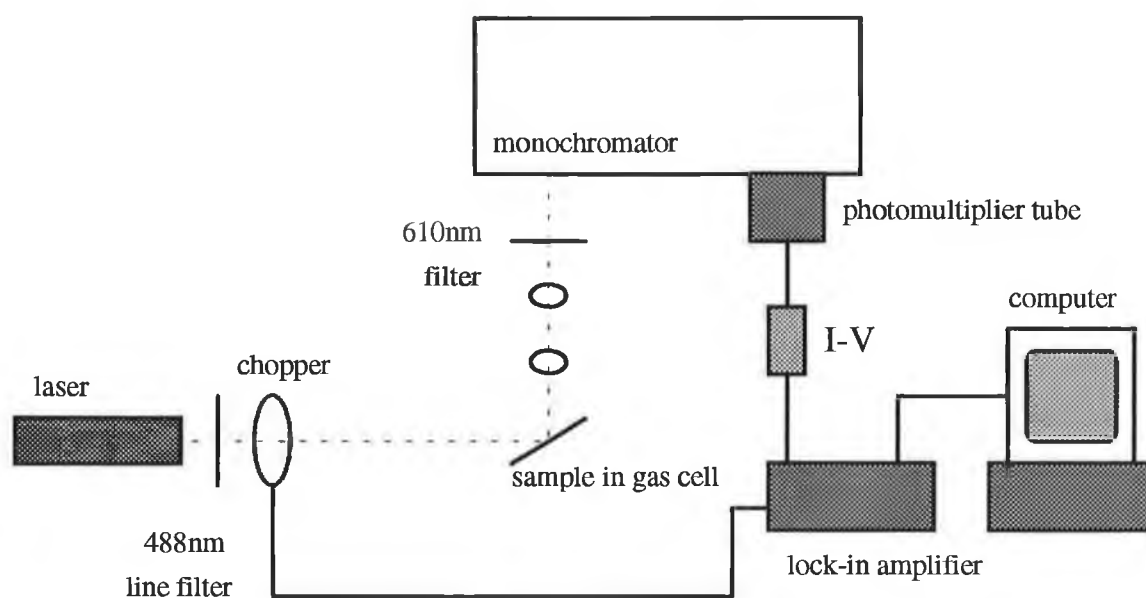


**Figure 4.5 Fluorescence Quenching Apparatus**

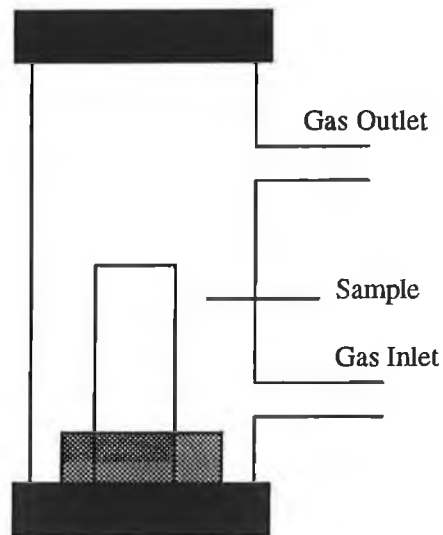


**Figure 4.6 The Gas Cell**

#### **4.6 Summary**

Details were given of sol-gel preparation techniques used in this work. The dip-coating apparatus was illustrated and the fabrication parameter variation within this experimental study was outlined. Finally film characterisation techniques and fluorescence measurement techniques were discussed.

#### **References:**

- [1] Brinker C.J., Scherer G.W., "Sol-Gel Science" Academic Press (1990).
- [2] Pope E.J.A., Mackenzie, J.D., "Sol-Gel Processing of Silica, II. The Role of the Catalyst" Journal of Non-Crystalline Solids 87, pages185-198. (1986)
- [3] Tompkins H.G., "A Users Guide to Ellipsometry" Academic Press, (1993).

[4] Rudolph Research AutoEL-III Ellipsometer, **Condensed Operating Instructions**

[5] Komatsu H. Prof., "**Interferometry: Principles and Applications of Two-Beam and Multiple-Beam Interferometry**", Nikon Technical Bulletin.

## **Chapter 5 Acid-Catalysed Films**

### **5.1 Introduction**

Films were fabricated using two different acidic catalysts, HCl and HF. The bulk of the work involved HCl with a sol pH of 1. A brief study was made of HCl films fabricated at pH=0.1 and pH=3. For all films, thickness and refractive index were monitored as a function of dip speed. Temporal behaviour of thickness and refractive index was also investigated. For HCl, pH=1 films, a comprehensive investigation was carried out on the variation of thickness and refractive index with water:TEOS ratio (R) and with ageing time. Surface quality of the films was also monitored. Only undoped films are dealt with here. Chapter 7 discusses some results on Ruthenium doped films.

### **5.2 HCl-catalysed (pH=1) films**

#### **5.2.1 Influence of the R value on film properties**

As discussed earlier (section 2.3.1), the molar ratio of water to TEOS (R) influences the structural evolution of sol-gel materials due to the role of water in the hydrolysis and condensation processes. Sols were prepared with pH=1, HCl as catalyst and ageing time of 5 hours at 70°C. R values were varied from 2 to 8.

Figure 5.1 shows thickness as a function of R for these films. All points are the average of 6 thickness readings, the standard deviation was 20nm. It is clear that increasing R leads to an increase in film thickness. At pH=1, hydrolysis is relatively fast compared to condensation, and as R is increased, the extra water promotes hydrolysis and is consumed[1]. This increase in hydrolysis results in thicker films. As R is increased further to the point where there is excess water over that required for

hydrolysis at a given sol pH, the extra water serves to dilute the sol by reducing relative silica content and giving rise to longer gel times and thinner films[2]. The latter behaviour is observed in the data of Almeida et al [3], where for films fabricated at pH=2.5, the gel times are considerably longer and the thickness decreases with increasing R value. In our work this point is reached at R=6 as shown on figure 5.1.

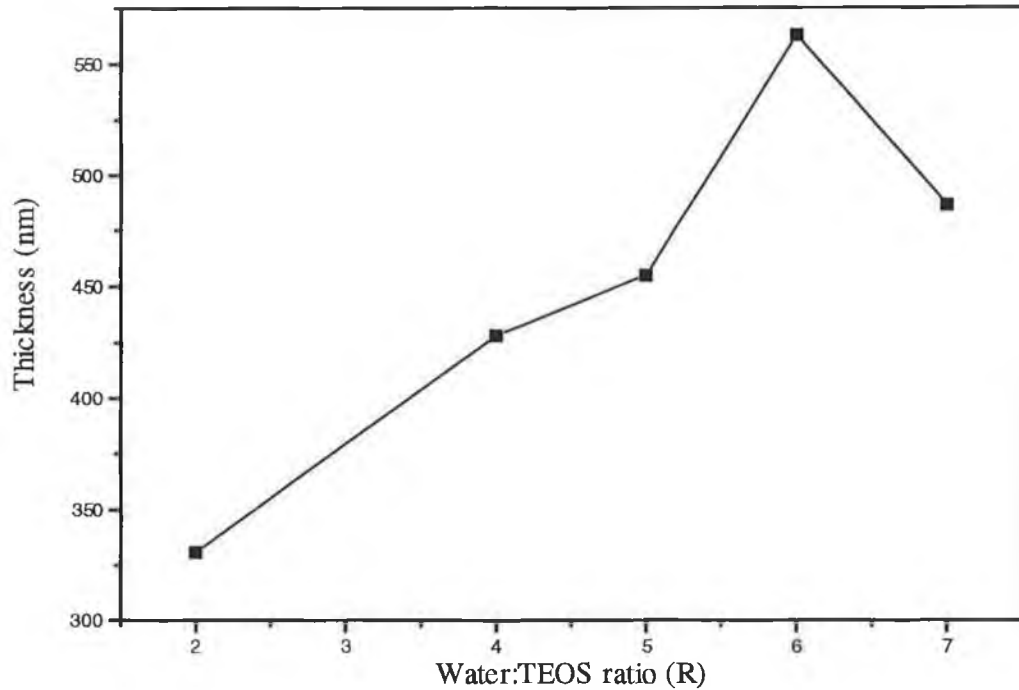


**Figure 5.1** The influence of water:TEOS ratio (R) on initial thickness

### 5.2.2 Influence of Ageing time on film properties

Sols were prepared and substrates coated as in section 5.1.1, but ageing times were varied. Ageing of the sol causes aggregation due to hydrolysis and condensation reactions, thus increasing the viscosity. Figure 5.2 shows film thickness as a function of ageing time for R=2, 4 and 6. The increase in thickness with ageing time for each R value is as expected and agrees with other studies[3]. As discussed in section 2.4.1, thickness is proportional to sol viscosity. Consequently the viscosity increase resulting from hydrolysis and condensation reactions which occur during ageing, gives rise to

thicknesses which increase with ageing time. For R=2 and R=4 sols, coating was possible without any ageing, but for R=6 this was not so. Gel times for R=2, 4 and 6 were 170 hours, 12 hours and 7 hours at 70°C respectively. The quality of the films deteriorated as ageing time approached the gel time due to the sol's high viscosity and inability to flow evenly over the substrate. Films produced from sols of high R values (R>6), were of poor quality due to the excess water which served to dilute the sol, (as discussed in section 5.2.3).

From figure 5.2 it is clear that the rates of change of thickness with ageing time for R=4 and R=6 are similar. For R=2 the rate of change is much slower. This behaviour is due to the relatively small amount of water and the consequent effect on sol properties.

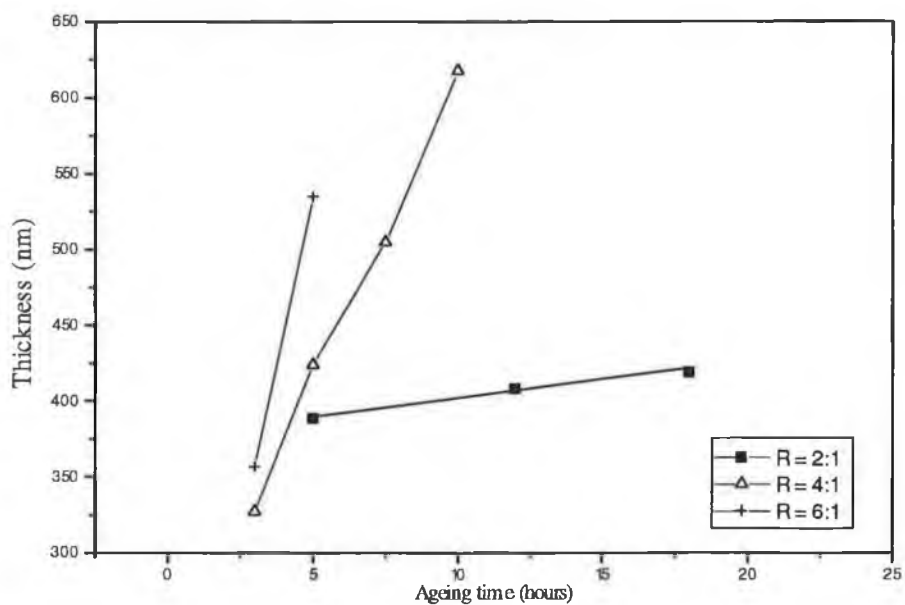


**Figure 5.2 Thickness versus Ageing Time for various R values**

### 5.2.3 Temporal behaviour of the films

Figure 5.3 shows the temporal evolution of film thickness after coating for R=2,4 and 6 films. Note that R=2 films had been aged for 18 hours while ageing time for the

other films was 5 hours, hence the larger initial thickness for R=2 films. It is obvious that films fabricated at the higher R value stabilise in a much shorter time. It was found that the thickness of films fabricated at R=2 decreased gradually over approximately 80 days, while for R=4 and R=6, the thickness stabilised in a shorter period of around 20 days.

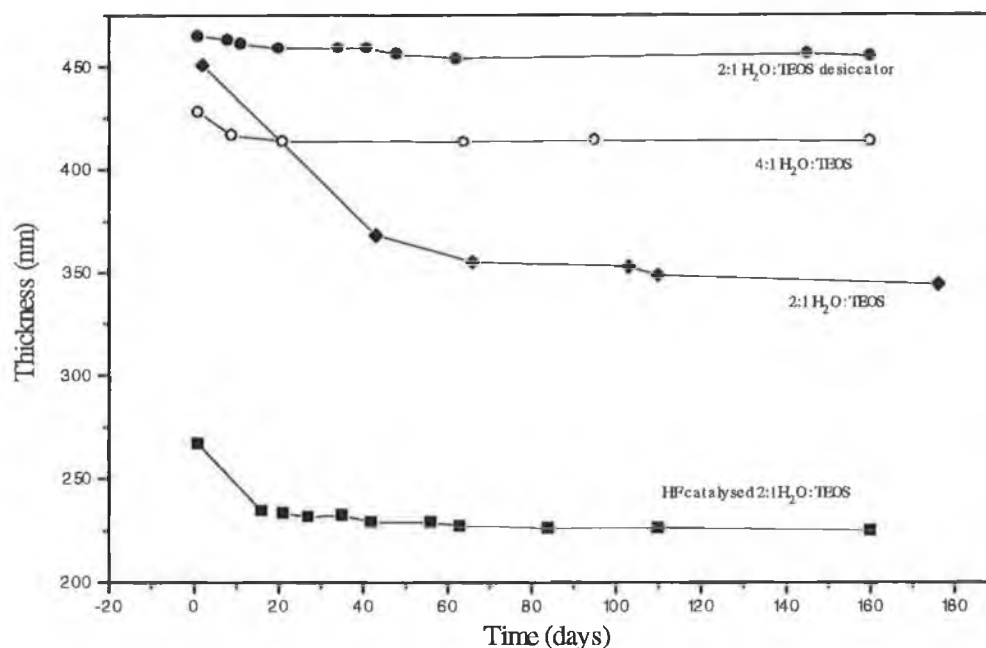


**Figure 5.3 Temporal behaviour of acid catalysed films: Thickness**

This is attributed to incomplete hydrolysis in the R=2 films, even though R=2 is the stoichiometric water:TEOS ratio. It is clear from the literature that, even at relatively high R values, unhydrolysed monomers can be present in the gel[4]. The result of this incomplete hydrolysis prior to coating is that, subsequent to coating, hydrolysis continues during the drying process, giving rise to a changing microstructure which causes a gradual decrease in film thickness. This continuing hydrolysis is facilitated by exposure to moisture in the atmosphere. An investigation into this theory involved measurement of thicknesses of R=2 films which had been stored in a desiccator after

drying. These measurements were compared to those of films stored under ambient conditions. The former remained approximately constant and compared well with values measured prior to storage as shown in figure 5.3. By subsequently storing these samples under ambient conditions thicknesses began to fall as they had done with the latter samples. These measurements are consistent with the theory of continuing hydrolysis in the presence of atmospheric moisture.

Investigations into the effect of ageing time on thickness stabilisation were carried out. It was found that for R=2, 4 and 6 increasing the ageing time gave rise to thicker films as seen previously but ageing had no effect on the stabilisation time as shown in figure 5.4 for R=2 films. This suggests that all films, regardless of processing conditions require at least 20 days for the thickness to stabilise.

To further investigate the stabilisation behaviour, the drying time was varied between 1 and 120 hours at 100°C for R=2 films. It was found that increasing drying time did reduce thicknesses of films. However, a duration of 80 days was still required for stabilisation and all thicknesses fell to approximately the same level as seen on figure 5.5, as for the standard drying time of 18 hours. In chapter 6, a similar investigation is reported for liquicoat films, where the same conclusion is reached, that drying time does not affect stabilisation time. The refractive index of the thin films was monitored over time as shown in figure 5.6. For R=4 it was found that refractive index remained approximately constant over time, whereas for R=2 there was a slight decrease in refractive index, which was independent of ageing and drying times. The refractive index decrease for R=2 films is unexpected. It appears from this investigation that films fabricated at R=2, pH=1 display some anomalous behaviour. The long stabilisation time attributed to continuing hydrolysis in the atmosphere, is accompanied by a decrease in refractive index which would indicate an increase in porosity as the microstructure changes over time. This behaviour illustrates the

variation in film properties achieved by adjusting relative hydrolysis and condensation rates.

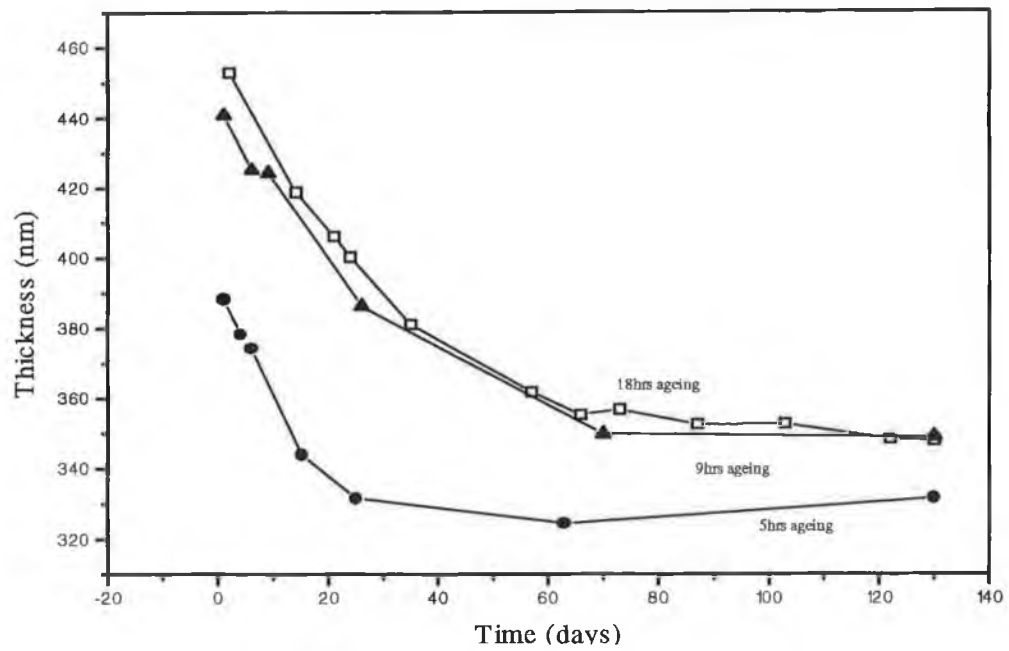


Figure 5.4 The influence of ageing time on temporal behaviour of thickness

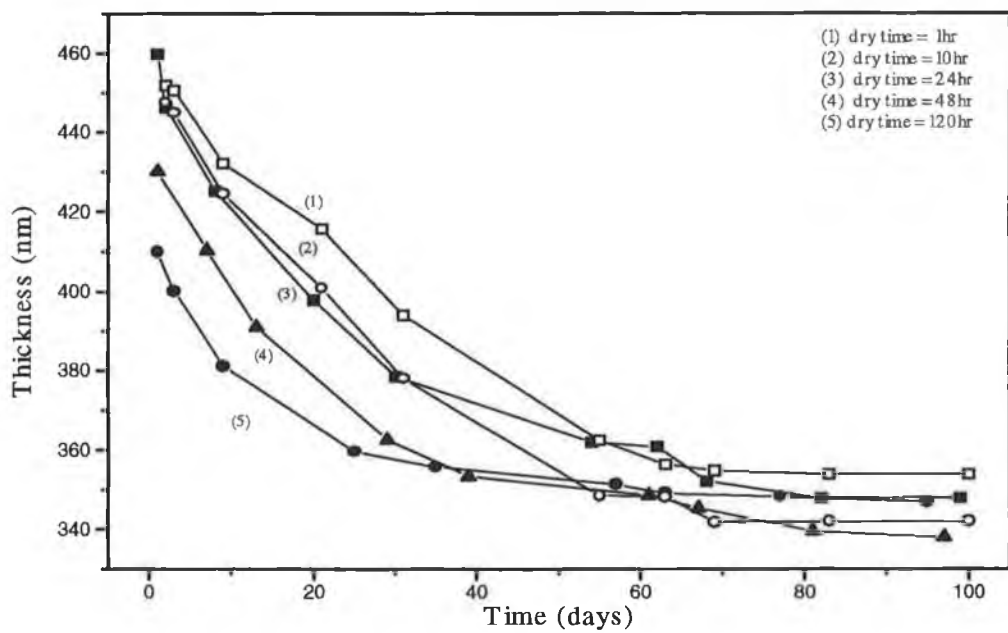
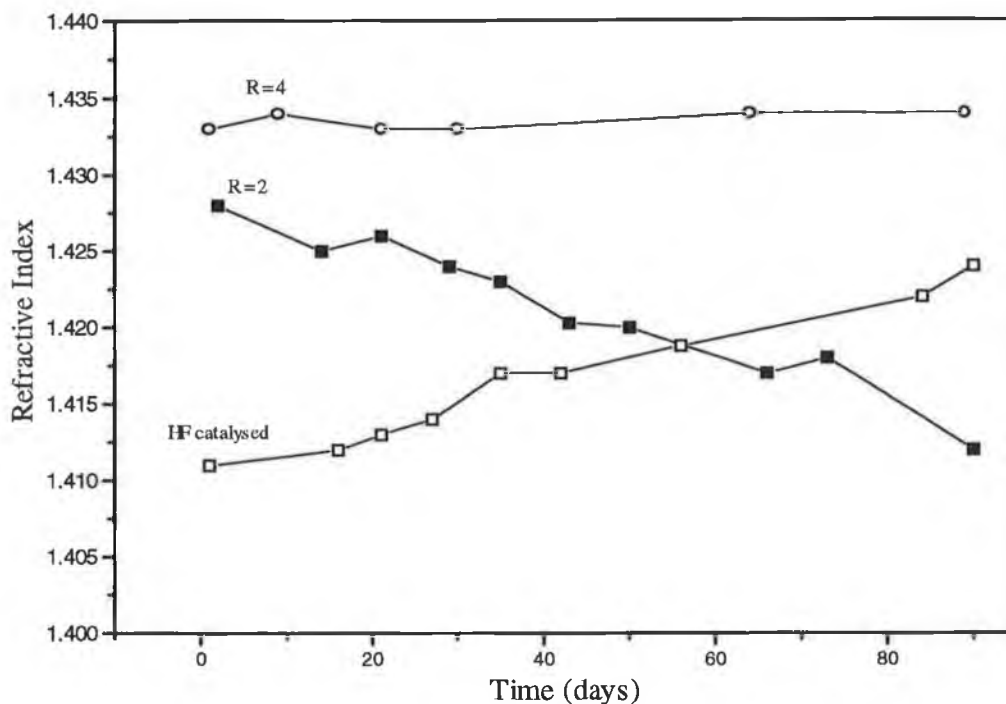


Figure 5.5 The influence of drying time on temporal behaviour of thickness



**Figure 5.6 Temporal behaviour of TEOS films: Refractive index**

#### 5.2.4 Influence of the Dipping Speed on film properties

As described in section 2.4.1, substrates were dip coated from sol solution. In this section an illustration of the effect of dipping speed on film characteristics will be given for films derived from sols of differing R values. Previous studies of dependence of film thickness on dipping speed[5] have reported slope values of between 0.5 and 0.65 for plots of  $\log(\text{thickness})$  versus  $\log(\text{dip speed})$ . Theory predicts either a slope of 0.5 or 0.66 depending on assumptions related to surface tension and viscosity dependence in equation 2.1.

Figure 5.7 presents corresponding data for TEOS-derived films made at pH=1 (HCl catalysis) and R=2,4,6 and 7. It is clear that the data is consistent with previous work apart from R=2 catalysed films which yield a slope  $\sim 0.4$  regardless of ageing time. Small deviations from predicted behaviour can be explained by such factors such as

non-Newtonian viscosity due to aggregation in the sol (especially after long ageing times) and concentration dependence of the viscosity due to evaporation. It is concluded that R=2 films deviated from predicted behaviour due to the relatively small amount of water reducing the efficiency of the hydrolysis and condensation reactions. This behaviour is consistent with other anomalous results for R=2 films as discussed above.

In conclusion, thickness can be tailored to a particular application by choosing a suitable dip speed. Generally as film thickness exceeded 600nm quality deteriorated, cracking and non-uniformity were evident.

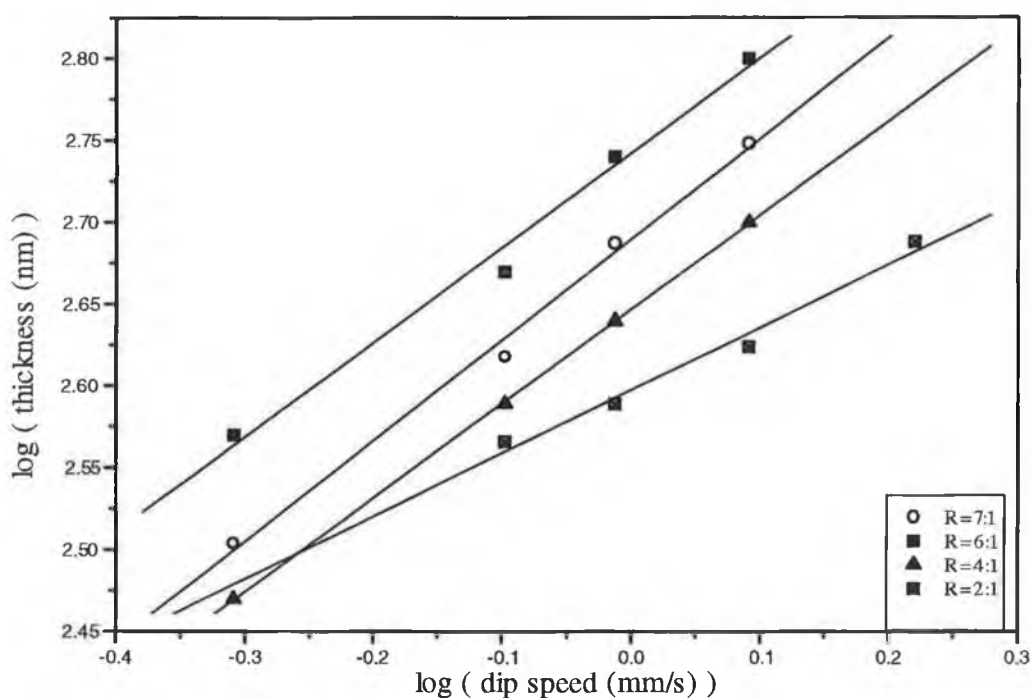


**Figure 5.7 Influence of dip speed on film thickness**

### 5.2.5 Summary

In this section HCl, pH=1 films have been discussed in terms of thickness, refractive index, temporal behaviour and quality resulting from parameter variations such as R-value, coating speed, ageing time and drying time. As R value increased from 2 to 6,

thicknesses of films produced increased due to enhanced reaction rates. However, as R value increased both film thickness and film quality decreased due to the dilution of the sol with the excess water.

Dipping speed variation was shown to facilitate variable thickness requirements. All films except those derived from sols of R=2 behaved as predicted by theory in terms. It was seen that as thicknesses went beyond 600 nm the quality deteriorated.

As ageing time increased so too did the thickness of the films produced. However, as ageing time approached the gel time, quality of the films deteriorated considerably.

The temporal stability (in terms of thickness and refractive index) of all the films except those derived from R=2 were characterised by a stabilisation time of approximately 20 days. R=2 films took approximately 80 days to stabilise. Both ageing and drying times had no effect on this behaviour.

## **5.3 Variation of pH**

### **5.3.1 HCl films fabricated at sol pH= 0.1 and pH=3**

The pH of the starting sol influences the hydrolysis and condensation rates as discussed in section 2.3.2. In this work thin films were fabricated from pH=0.1 and 3, using R=2 sols, with HCl as catalyst. All these films were dried at 70°C for 18 hours as for pH=1. Table 5.1 shows the initial thicknesses and gel times of the films formed. pH=3 films are very thick when compared to pH=1 and to pH=0.1. This is as expected from figure 2.3. At pH=3, condensation is fast relative to hydrolysis and this results in rapid cross-linking with water and alcohol as by-products. The water produced is used in hydrolysis and compensates for the low R value (section 2.3.1). Due to this, viscosity increases relatively rapidly, gel time is shortened and the thickness of films produced is increased.

For pH=1, hydrolysis is the predominant reaction, which is limited by the low R value (R=2). Gelation time is thus increased, the sol produced is less viscous at a given time and films produced have a decreased thickness.

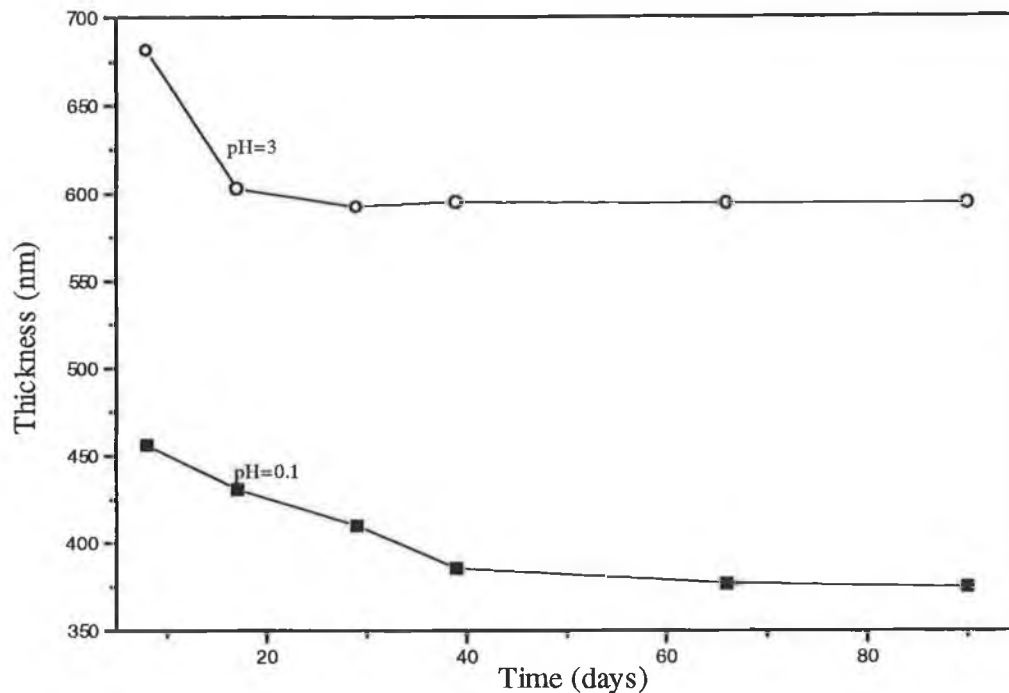
For pH=0.1, condensation rates are between those of pH=1 and pH=3, hydrolysis is much faster due to greater acidity and the resulting gel time is intermediate between the other pH values examined. Thus initial thickness is lower than that of a pH=3 film but thicker than that of pH=1.

pH	Thickness	Gel-time
pH=1	450nm	170 hours
pH=0.1	500nm	120 hours
pH=3	700nm	80hours

**Table 5.1 Gel-times of sols of various pH**

### 5.3.2 Temporal Stability

The thicknesses of the films made from sols of pH=3 and pH=0.1 were measured over time. With reference to figure 5.8, it can be seen that pH=3 sol-gel films stabilised within 20 days like films made from sols of higher R-values (section 5.2.3). The enhanced condensation for pH=3 accounts for this. In the basic regime enough water is produced as a by-product to compensate for the low R values, thus completing hydrolysis well in advance of a pH=1, R=2 sol. Films made from pH=0.1 sols have a longer stabilisation time, similar to that of R=2, pH=1 films. Where pH=0.1, the reactions are acid-catalysed and hydrolysis is the dominant process. Hydrolysis processes continue long after dipping using water in the atmosphere.



### 5.8 Temporal behaviour of pH varied HCl, 2:1 films: Thickness

### 5.4 HF-catalysed films

As discussed in section 2.3.4, film properties are affected by the catalyst type as well as pH. In this work a comparison is drawn between films formed from HF-catalysed sols and those of HCl-catalysed sols. A sol with R value of 2 but catalysed with HF was made. The gel time of this sol was 1.5 hours at 70°C, compared to a HCl sol which has a gel time of approximately 170 hours at the same temperature. Due to this, the HF sol was aged for 24 hours at room temperature and then coated onto substrates. The thickness of the films formed was lower (250 nm) than those of the standard HCl films (sol ageing 18 hrs@70°C). The fast gel time reflects the catalysis mechanism involved, whereby the fluorine ion serves to catalyse both the process of hydrolysis and condensation[4,6] and produces gels which are similar in character to base-catalysed gels.

The temporal stability of thickness and refractive index was measured. It was found that, as with films fabricated from R=4 and 6 (HCl catalysed, pH=1), the thickness stabilised after just 20 days as is shown in figure 5.3. Over the same period the refractive index increased as expected as shown in figure 5.6. The continuing processes of hydrolysis and polycondensation cause cross-linking of the sol network, expelling solvents and water to result in an increase in density. This faster stabilisation is indicative of a sol which is more advanced at the point of dipping than that of the HCl-catalysed, R=2 sol.

## 5.5 Summary

Results from experiments on acid-catalysed films have been detailed in terms of thickness, refractive index, temporal behaviour and quality. Parameters varied included R-value, ageing time, pH, catalyst type and dip-coating speed. In summary, the R value in HCl catalysed films of pH=1 influences properties such as quality, thickness and temporal evolution of films. R=4 sols which were aged for 5 hours produced the better quality and stabilisation characteristics, when compared to films made from sols with other R values.

pH studies showed that pH=3 sols produced thicker films after a given ageing time than others of shorter stabilisation time, although quality was poor. pH=0.1 had temporal behaviour and quality similar to pH=1. For future work it may prove beneficial to make sols of pH=3 with a shorter ageing time. It is expected that this would improve the quality, while still maintaining the relatively short stabilisation time.

HF was used to catalyse R=2, pH=1 sols. Films produced were superior in quality when compared to any of the above. Films were seen to stabilise in a manner similar to those of the higher R values in HCl catalysed sols. Processing has the capability of

being relatively short due to the fast gelling time of the sol. However with all of this in mind HF is hazardous to use.

Coating speed has been shown to facilitate various film thicknesses as all films were seen to have an increase in thickness with increasing dipping speed.

### **References:**

- [1] Pouxviel, J.C., Boilet, J.P., Beloeil, J.C., Allemand, J.Y., Journal of Non-Crystalline solids, 89 345, (1987).
- [2] Klein, L.C., Annual Review of Material Science, 15, 27, (1985)
- [3] Almeida, R.M., " **Influence of processing parameters on the thickness of the sol-gel silica films**", Journal of Optoelectronics, 9(2) 135, (1994)
- [4] Brinker, C.J., Scherer, G.W., "**Sol-Gel Science**", Academic Press, (1990).
- [5] Strawbridge, I. and James, P.F., Journal of Non-Crystalline Solids, 86, 381, (1986).
- [6] Pope, E.J.A. and Mackenzie, J.D., "**Sol-gel processing of Silica II. The role of the catalyst.**", Journal of Non-Crystalline Solids, 87, pages 185-198, (1986).

## **Chapter 6 Liquicoat-derived Thin Films**

### **6.1 Introduction**

As described in section 4.4.2 commercial silica and titania sol-gel solutions were used to prepare silica and silica/titania thin films. These films were characterised and compared to one another and to TEOS based sol-gels. In this chapter details on both silica films and silica/titania films will be given. Characteristics studied were the influence of dip speed on refractive indices and thicknesses, the temporal behaviour of the films and the film quality. From films made with various silica/titania combinations, samples of varying refractive indices could be made. All films dealt with in this chapter are undoped. Doped liquicoat samples are characterised in Chapter 7.

### **6.2 Silica Liquicoat**

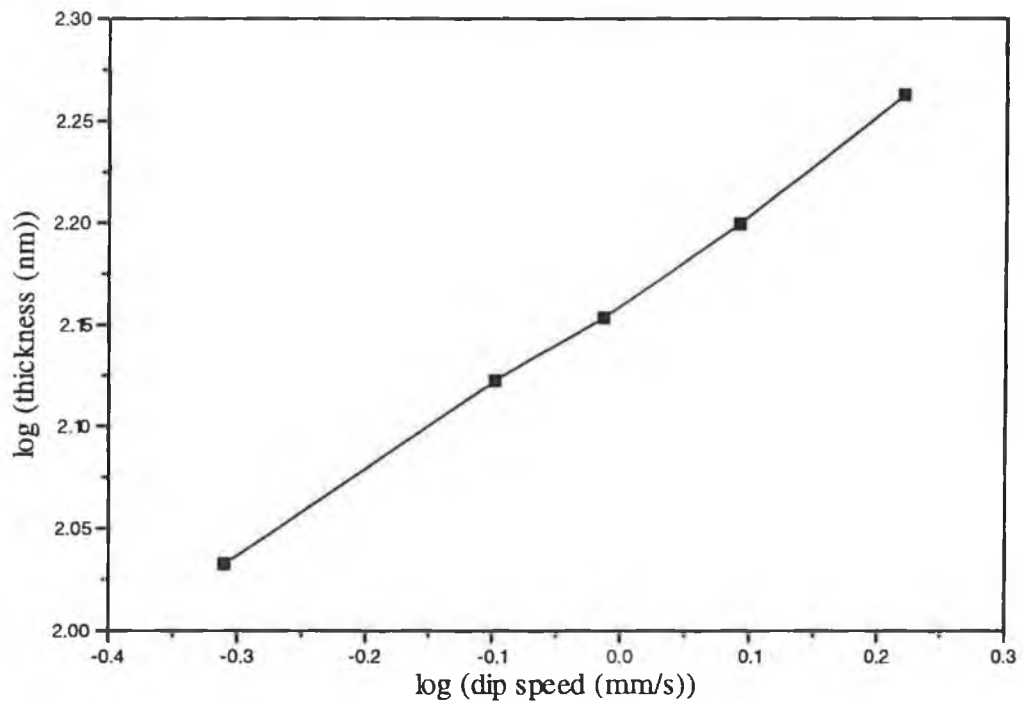
#### **6.2.1 Dip Speed versus Thickness and Refractive Index**

Figure 6.1 presents the graph of  $\log(\text{dip speed mm/s})$  versus  $\log(\text{thickness nm})$ . This graph has a slope  $\sim = 0.5$ . With reference to section 2.4.1 it is clear that this agrees with theoretical predictions for Newtonian fluids and is similar to the behaviour of TEOS-based films. The refractive index of silica liquicoat films decreased slightly with increased dip speed. This is to be expected as a thicker film will dry more slowly resulting in a larger porosity and lower density.

#### **6.2.2 Temporal Stability**

Temporal behaviour of the thickness of silica liquicoat films is seen in figure 6.2, and of refractive index in figure 6.3. The thickness and refractive index are seen to

stabilise (within the standard deviation of 20nm) within 20 days of drying. The behaviour is consistent with that of all TEOS (pH=1) slides except for that of R=2 (HCl, pH=1). In an effort to reduce this stabilisation time the drying time influence was investigated. The recommended drying time was 10 minutes at 100°C as discussed in section 4.2.2. In this work slides were dried for times ranging between 10 minutes and 3 hours. On monitoring the thickness over time, it was established that the stabilisation time was not affected, as shown in figure 6.4. This corresponds to a similar study carried out on the standard (HCl catalysed, pH=1, R=2) slides reported in Chapter 5.



**Figure 6.1 Dip speed versus film thickness: SiO<sub>2</sub> liquicoat**

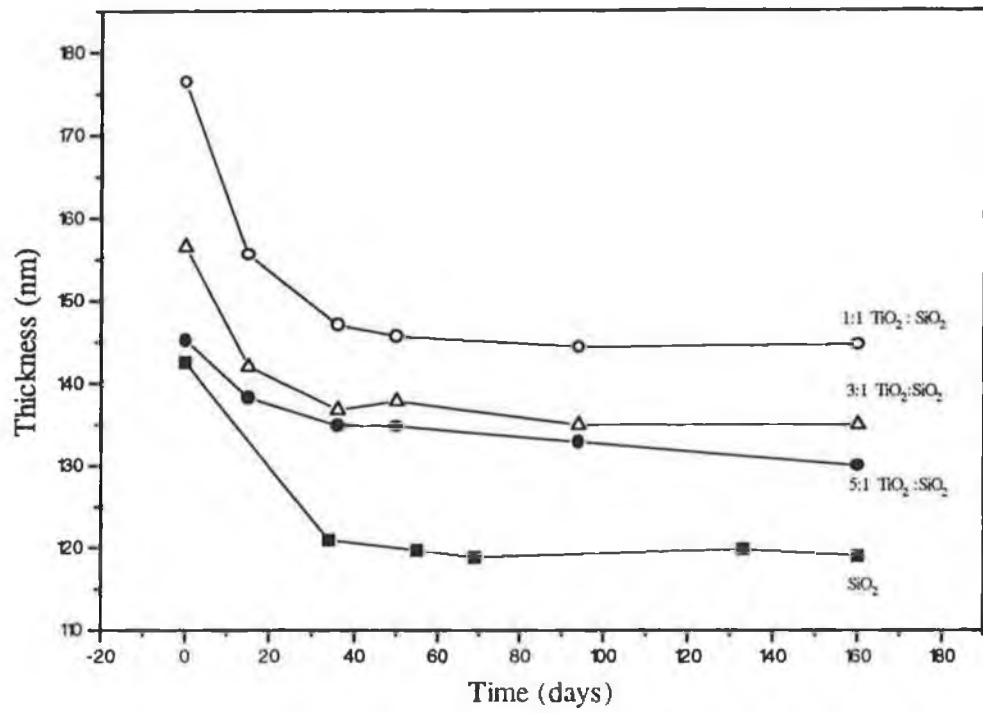


Figure 6.2 Temporal behaviour of liquicoat films: Thickness

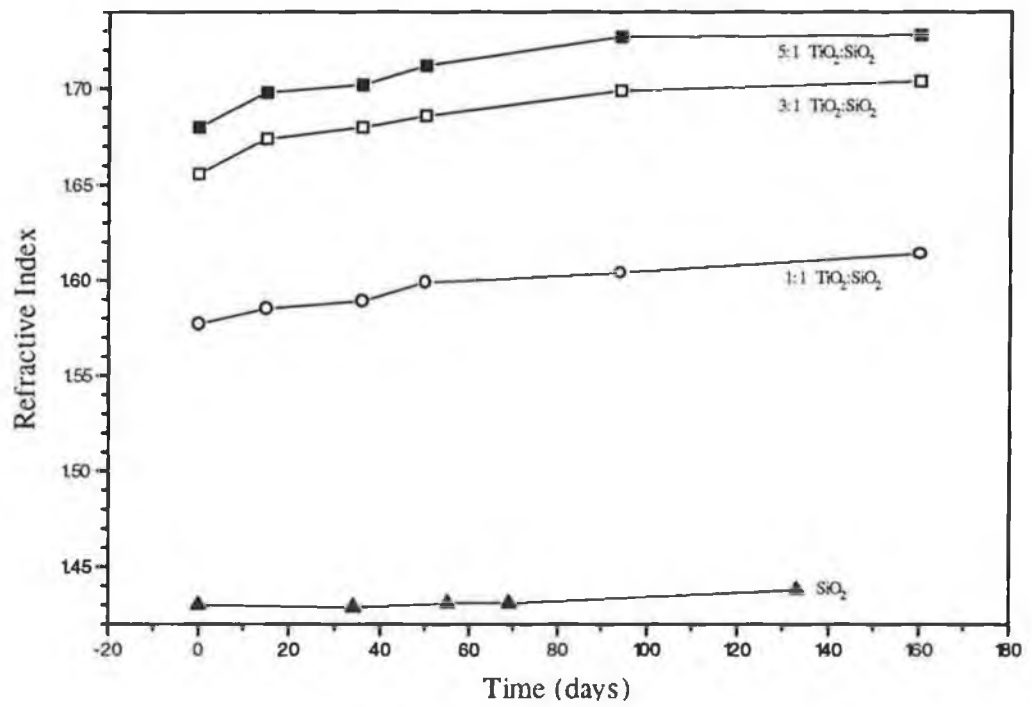
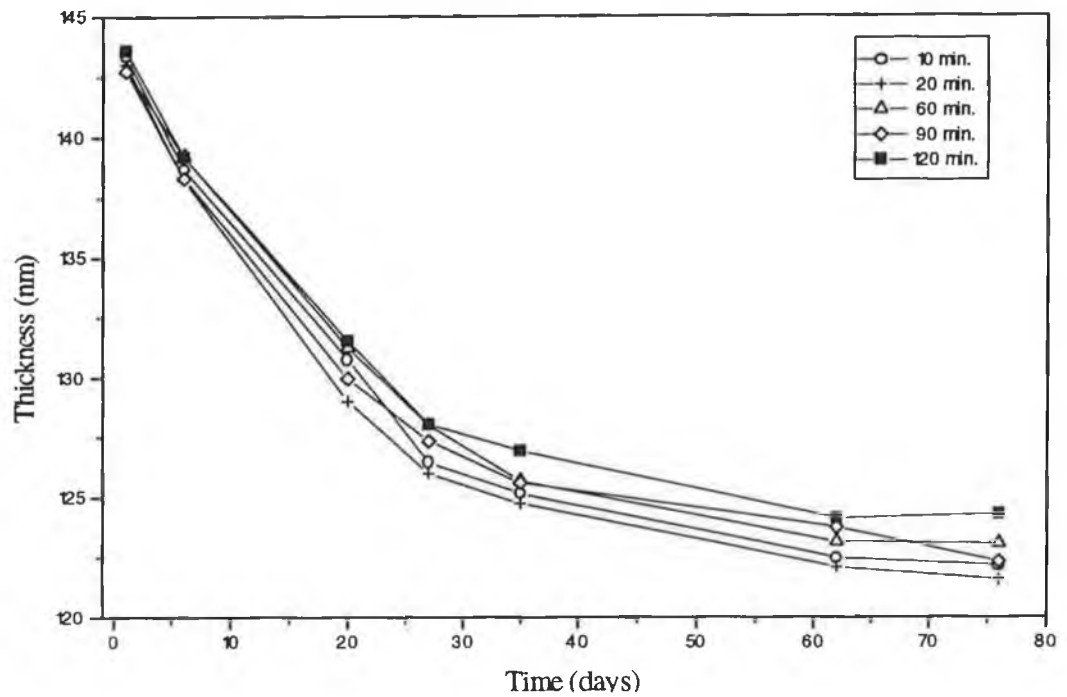


Figure 6.3 Temporal behaviour of liquicoat films: Refractive index



**Figure 6.4 Temporal behaviour of SiO<sub>2</sub> liquicoat films after various drying times**

### 6.3 Silica/Titania Liquicoat Films

Silica: Titania mixes were made as described in section 4.2.2. They were characterised similarly to the silica films. Silica/titania mixes offer the facility of tailoring refractive index for a specific purpose.

#### 6.3.1 The influence of Dip Speed on Film Thickness and Refractive Index

As with silica films the graph of log (dip speed mm/s) versus log(thickness nm) yields a slope of ~ 0.5, this can be seen in figure 6.1. and corresponds to theory [1].

### 6.3.2 Refractive Index Behaviour

For  $\text{SiO}_2/\text{TiO}_2$  mixtures spanning between the range of 0.25  $\text{TiO}_2$  to 0.85  $\text{TiO}_2$  it can be seen in figure 6.5 that refractive indices range from 1.42 for porous silica to ~2 for a porous undensified titania film. The relationship is clearly linear. The availability of this variable-index facility enables the optimisation of wave-guide structures for optical sensors [3].

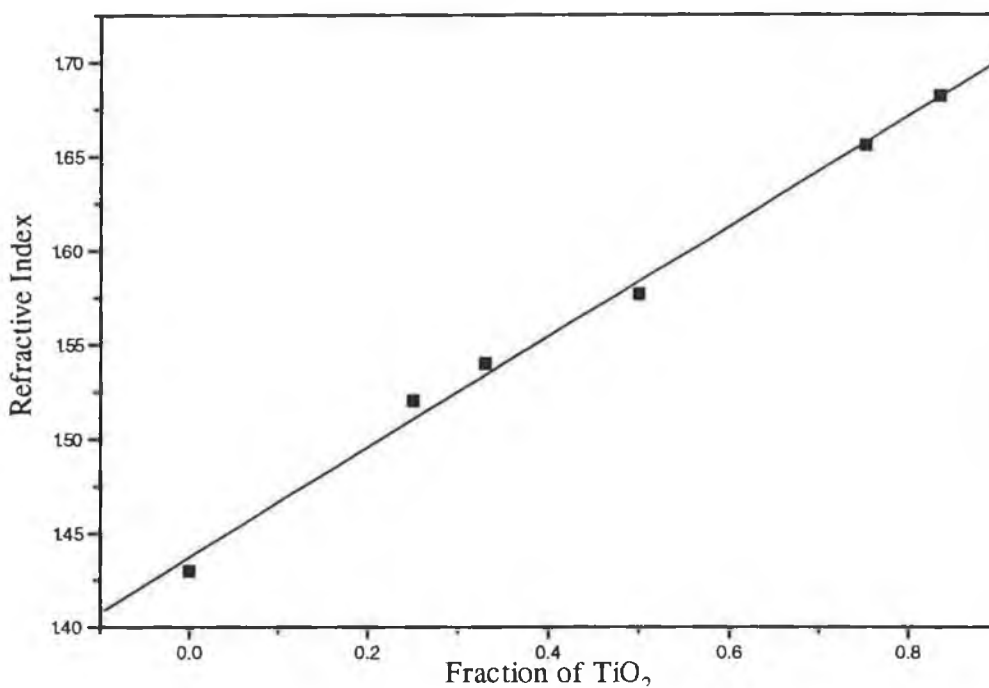
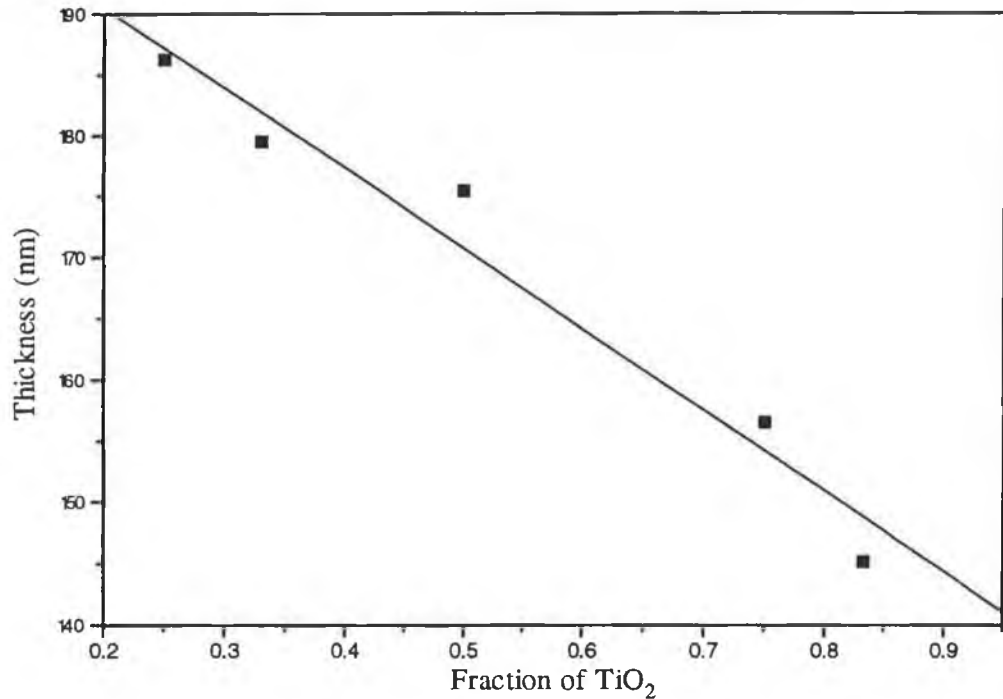


Figure 6.5 Refractive index as a function of titania content

### 6.3.3 Thickness behaviour

Silica and silica/titania mixes produced films of variable thicknesses, much lower than those of the standard HCl catalysed, TEOS films. Silica films were thinner than those from silica/titania sols, this implies that the viscosity of the latter is greater, however it can be seen from figure 6.6 that thickness of the silica/titania films decreased as titania

content increased. It is clear that there is a complex viscosity behaviour in the liquicoat mixtures which gives rise to an all-silica film having a smaller thickness than the silica/titania mixtures, but meanwhile thickness also decreases with titania content.



**Figure 6.6** Thickness as a function of titania content

#### 6.4 Surface Quality

In general the surface quality of liquicoat sample films was superior to those of the standard TEOS derived (excluding HF catalysed) films. Although the latter were crack-free, except for those produced at long ageing times, film thickness was non-uniform at the edges while all liquicoat films (except titania-only films) exhibited superior film thickness homogeneity.

## 6.5 Summary

In this chapter, results from experimental work with liquicoat-derived films are given. Liquicoat films followed theoretical predictions in terms of thickness change with dipping speed. Refractive index decreased slightly with increasing dip speed but in a more linear way than for TEOS R=2 films. Temporal behaviour of thickness was similar to that of HF catalysed and HCl catalysed (R>2) films. The facility of variable refractive index with SiO<sub>2</sub>:TiO<sub>2</sub> mixes was illustrated. Surface quality was seen to be excellent relative to TEOS-derived, except in the case of TiO<sub>2</sub> films. Although films were of good quality, it will be seen in the following chapter that when doped with ruthenium complex, the behaviour is not as good as that of TEOS based films mainly because the dye leaches out of the films over time due to larger pore sizes which are characteristic of particulate sols which is the basis of the Liquicoat solution.

## References:

- [1] Strawbridge, I. and James, P.F., Journal of Non-Crystalline Solids, 86, 381 (1986)
- [2] Brinker, C.J. and Scherer, G. W., "**Sol-Gel Science**", Academic Press (1990).
- [3] McCulloch, S., Stewart, G., Guppy, R.M. and Norris, J.O.W., "**Characterisation of TiO<sub>2</sub>-SiO<sub>2</sub> sol-gel films for optical-chemical sensor applications**" Journal of Optoelectronics, volume9, number 3, pp 235-241 (1994).

## Chapter 7 Quenching behaviour of Ruthenium doped films

### 7.1 Introduction

In order to investigate the behaviour of sol-gel films in optical oxygen sensing, films were made which were doped with  $\text{Ru}(\text{Ph}_2\text{phen})_3\text{Cl}_2$  and put through a series of tests as described in section 4.2.

### 7.2 Quenching of Fluorescence

As discussed in Chapter 3, fluorescence from the ruthenium complex is quenched in the presence of oxygen. The fluorescence intensity is thus a measure of oxygen concentration as expressed in equation 7.1, the Stern-Volmer relationship. This is the basis of optical oxygen sensing using ruthenium doped sol-gel films. In this chapter, the quenching behaviour of HF-catalysed films and liquicoat films are discussed as well as that of HCl-catalysed films. The relevant parameter which was measured was the quenching response,  $Q$ , defined as

$$Q = (I_{\text{N}_2} - I_{\text{O}_2}) / I_{\text{N}_2} \quad (7.1)$$

where  $I_{\text{N}_2}$  is the intensity measured in 0% oxygen (i.e. 100%  $\text{N}_2$ ) and  $I_{\text{O}_2}$  is that which was measured in 100% oxygen.

In this work quenching behaviour was investigated in terms of  $Q$  and response as a function of oxygen concentration.

### 7.3 Acid catalysed films

Films fabricated using a sol in which  $R=2$ , and HCl was the catalyst were studied previously[1], and seen to initially display a quenching response of 98%. However

this quenching response decreased to 80% over 80 days, corresponding to the period necessary for thickness stabilisation of the films. These films were very sensitive in the range of small oxygen concentrations and the response becomes more linear at higher oxygen concentrations as shown in figure 7.1.

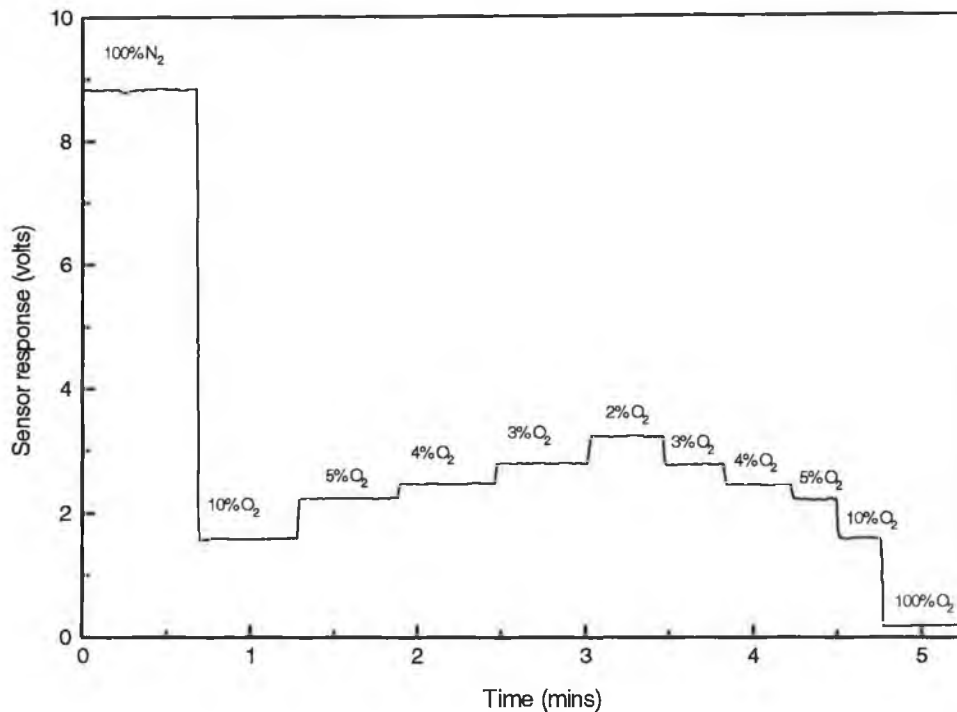


**Figure 7.1 Quenching behaviour as a function of oxygen concentration: HCl,**

**2:1**

In this work oxygen quenching of films made from sols of  $R=2$  which were catalysed with HF were investigated. It was found that after coating the quenching response was 90%, however the thickness of the film had not stabilised at this point, (refer to section 5.2.3). When the quenching experiment was repeated subsequent to thickness stabilisation, quenching was 70% on average. The response to alternate environments of 100% nitrogen to 100% oxygen is shown in figure 7.2. The response compares favourably with HCl data[1]. Figure 7.3 shows the intensity as a function of oxygen

concentration. While there is an inherent non-linearity in the oxygen response as seen

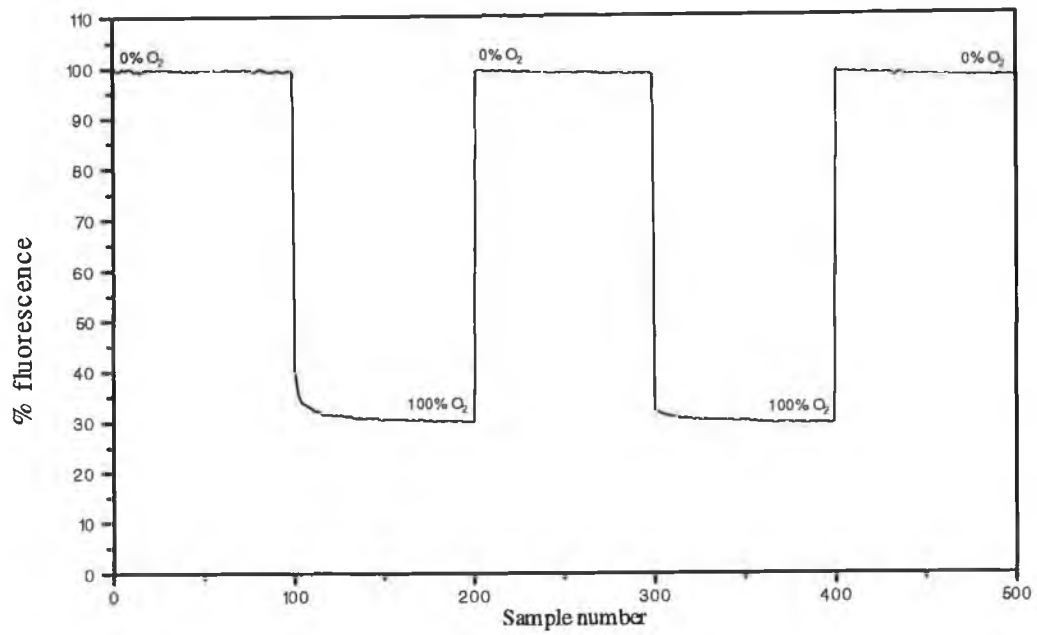


**Figure 7.2** Quenching response to oxygen: HF-catalysed 2:1 film

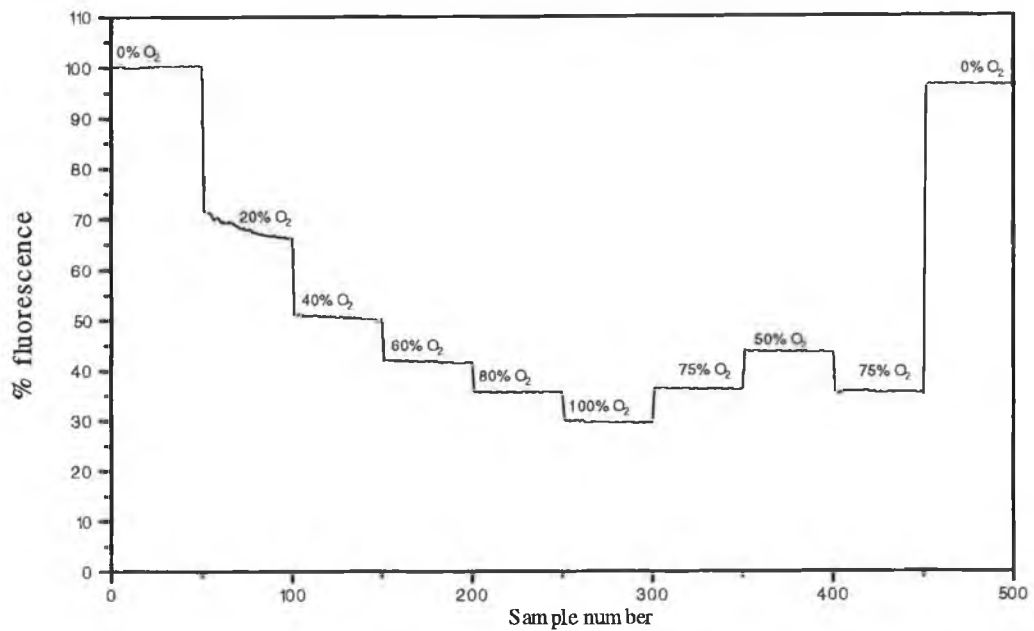


**Figure 7.3** Quenching as a function of oxygen concentration: HF-catalysed film

in the Stern-Volmer equation (7.1), there is also a clear variation in the linearity as a function of oxygen concentration for different films. It is clear from figures 7.1 and 7.3 that HCl-catalysed films have a greater sensitivity at low oxygen concentrations compared to HF-catalysed films. This variation is thought to be related to the different  $O_2$  diffusion rates in films with different pore sizes. Figure 7.4 shows Stern-Volmer plots for HF-catalysed and silica liquicoat. The corresponding plots of intensity versus oxygen concentration for these films are shown in figures 7.3 and 7.5 respectively. Referring to equation 3.2, the Stern-Volmer equation, the slope in figure 7.4 represents  $K_{SV}$ , the Stern-Volmer coefficient. Since  $K_{SV}$  is directly proportional to  $D$ , the diffusivity through the medium, it is clear that HF-catalysed films have larger diffusivity than the silica liquicoat films. It is expected that this should also be the case in HCl-catalysed stable films, refer to section 2.3.4. The diffusion is related to the average pore size in the film so this result is consistent with the larger pore sizes of HF-catalysed films compared to liquicoat films. This effect is still under investigation.

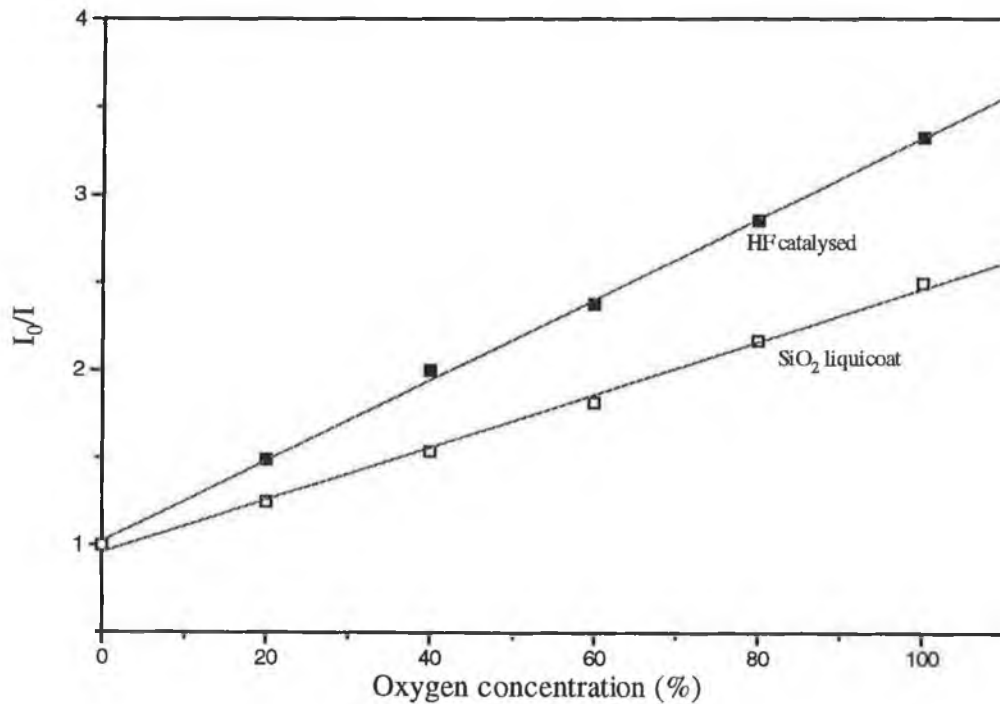


**Figure 7.4 Stern-Volmer plots for HF-catalysed and liquicoat films**

## 7.4 Liquicoat Films

### 7.4.1 SiO<sub>2</sub> liquicoat films

SiO<sub>2</sub> liquicoat was doped with an amount of Ru(Ph<sub>2</sub>phen)<sub>3</sub> equivalent in weight to 20,000ppm in TEOS sols. Films were fabricated and their quenching response was investigated prior to thickness stabilisation. Films displayed on average 85% quenching response which decreased to 60% on stabilisation. The quenching behaviour as a function of oxygen concentration is shown in Figure 7.5. Its Stern-Volmer plot is in figure 7.4. It is clear that on comparison with TEOS based films the SiO<sub>2</sub> liquicoat films are not as sensitive to low oxygen concentrations due to the differing microstructures.

SiO<sub>2</sub> films doped with 8 times the concentration of Ru(Ph<sub>2</sub> phen)<sub>3</sub>Cl<sub>2</sub> used above were fabricated. They displayed a total quenching response of 97% initially, over the stabilisation time this fell to 70%, shown in figure 7.6. Initially the change in quenching as function of oxygen concentration was highly non-linear, showing a response of 70% between 0% and 20% oxygen. Over time this response became more linear. On comparison with films of lower dopant concentrations these stabilised quenching responses were larger. This difference between films with different dopant concentration reflects a change in microstructure due to the influence of ruthenium

concentration.

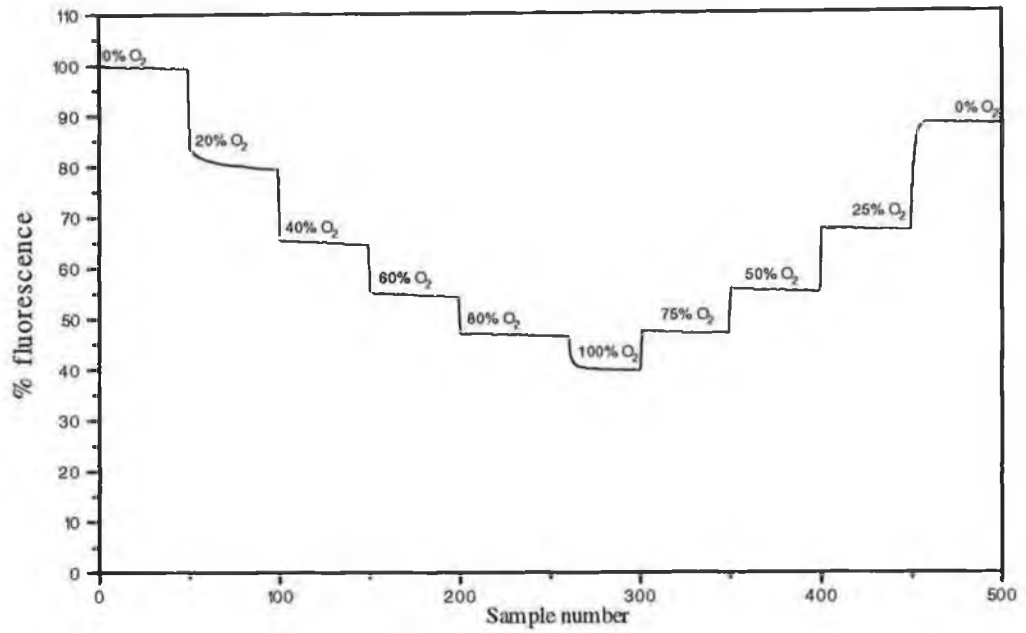


Figure 7.5 Quenching as a function of oxygen concentration: SiO<sub>2</sub> liquicoat

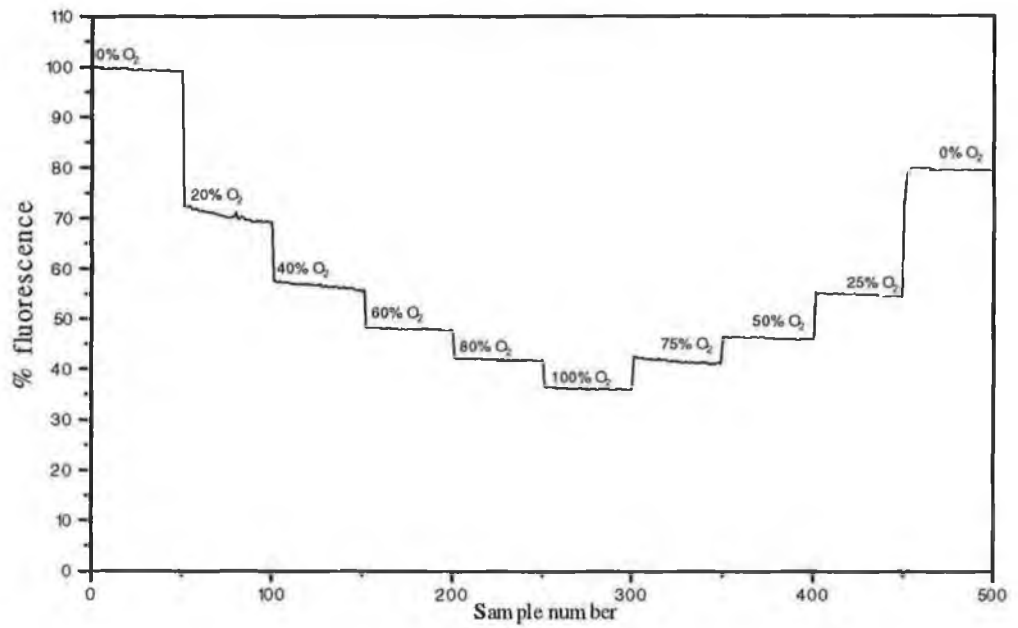
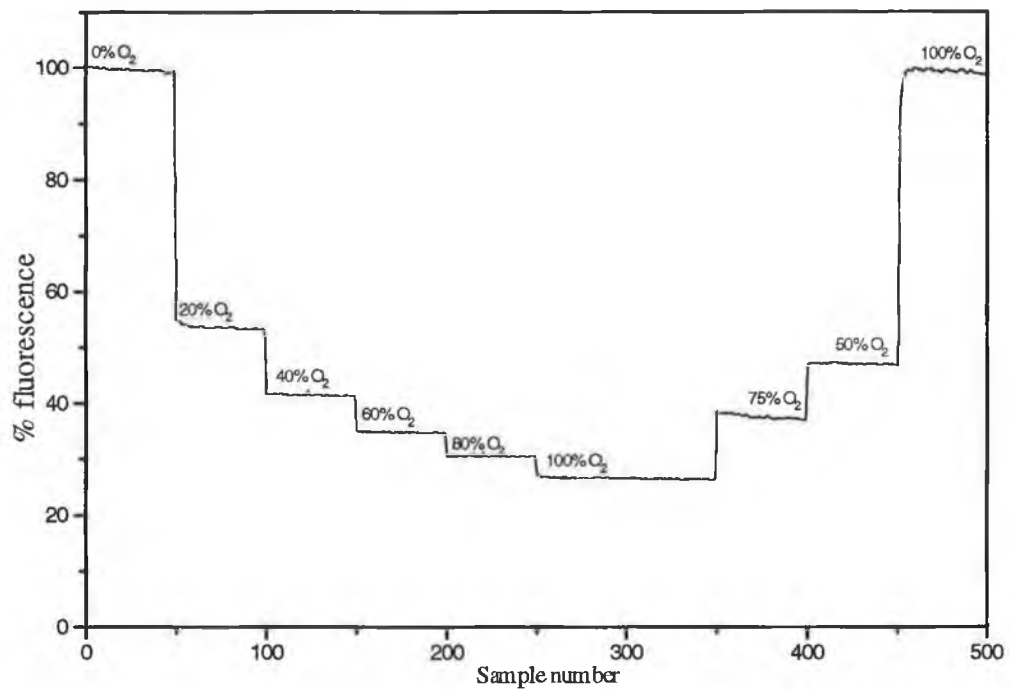


Figure 7.6 Quenching as a function of oxygen concentration: highly doped SiO<sub>2</sub> liquicoat

### 7.4.2 SiO<sub>2</sub>/TiO<sub>2</sub>

SiO<sub>2</sub>:TiO<sub>2</sub> liquicoat was mixed with a ratio of 1:1 as described in section 4.2.2, and then coated onto glass substrates. Quenching was examined and seen to change over the time required for the stabilisation of thickness, as found for other films. Initially quenching was approximately 90%, over time it fell to approximately 75% as seen in figure 7.5. The response as a function of oxygen concentration seen in figure 7.5, was similar to that of the HF-catalysed sols in terms of its non-linearity as seen in figure 7.3. It showed greater sensitivity in lower oxygen concentrations than in higher, see figure 7.9. However in comparison to HCl[1] films its overall quenching response is low.



**Figure 7.7** Quenching as a function of oxygen concentration: SiO<sub>2</sub>:TiO<sub>2</sub> 1:1 liquicoat

## 7.5 Intensity fall-off

Some photobleaching, observed as a fall off in intensity over time, was evident in all of these samples. The fluorescence was excited with an argon ion laser of power output 5mW. In a sensor configuration, excitation is by a blue LED which has a lower power output and hence photobleaching is minimised.

## 7.6 Summary

Sol-gel thin films derived from TEOS and liquicoat were doped with an oxygen sensitive ruthenium complex and their response to gaseous oxygen was investigated. All films displayed high fluorescence quenching responses when tested soon after fabrication. Corresponding to their thickness stabilisation discussed in chapters 5 and 6, their quenching response decreased over time. This illustrates the dependence of quenching behaviour on the sol-gel film microstructure. As the films densify and decrease in thickness the oxygen sensitive dye becomes less accessible to the gas and sensitivity is reduced. The variation in quenching as a function of oxygen concentration is attributed to different diffusion behaviour due to the different pore sizes in the different films. This effect is currently under investigation.

In all of the films examined there was a fall-off in intensity over time, this was attributed to photobleaching of the dye to the relative high laser excitation intensity.

In conclusion, stabilised films of HCl and HF-catalysed sols, and SiO<sub>2</sub>/TiO<sub>2</sub> liquicoat showed similarly high quenching responses of 80%, 70% and 75% respectively. SiO<sub>2</sub> liquicoat films displayed a quenching response of 60%, which was relatively low. However in quenching response as function of oxygen concentration these films displayed greatest linearity, SiO<sub>2</sub>/TiO<sub>2</sub> films showed large sensitivity to small

concentrations of oxygen. HF and HCl films stood somewhere in between. The different diffusion of oxygen in the different microstructures is thought to influence this.

### **References:**

[1] McEvoy, A., School of Physical Sciences, Dublin City University, Personal communication.

[2] Stern, O., Volmer, M., M.Phys.Z. 20,183.(1919)

## **Chapter 8 Concluding Remarks**

### **8.1 Overall Summary and Conclusions**

Films were fabricated under different conditions. Thickness, refractive index, oxygen sensing behaviour and surface quality were monitored. For the most part, the investigation focused on HCl catalysed films fabricated at pH=1. The flexibility of the sol-gel process was demonstrated by the large variation in thickness achievable by varying the water:precursor ratio, ageing time and dip speed. The results of the R value variation and temporal behaviour of thickness give an insight into the complex hydrolysis and condensation reactions which together determine the final structure of the film. In this work the influence of the R value on hydrolysis and condensation was clearly demonstrated by the thickness behaviour as a function of R and the anomalous behaviour of R=2 films. The results for HF-catalysed films demonstrated the effect of using different catalysts. Liquicoat solutions offer a fast, convenient method of film fabrication, but they do not have the same flexibility of being able to tailor film properties, for example porosity, for specific applications.

### **8.2 Optimisation of film for oxygen sensing**

This work has made a considerable contribution to the task of choosing optimum fabrication conditions for films for oxygen sensing. Currently the films being used for optical sensing in this laboratory are HCl-catalysed, pH=1, with R=4. These films stabilise relatively quickly and are of good optical quality, while R=4 gives a porosity sufficient for entrapment of the ruthenium complex without leaching, while ensuring accessibility of gases. From this work it is concluded that HF-catalysed films are equally suitable from the point of view of quenching response and are of superior

optical quality. However, so far, it is considered that HCl is safer and more convenient to use than HF. Liquicoat films are also of superior optical quality to HCl films, but they do not offer the facility of being able to tailor the microstructure.

### **8.3 Achievement of Objectives**

With reference to section 1.5, all the objectives of the project have been achieved. Furthermore the work has made a considerable contribution to the optimisation of sol-gel films for optical sensing.

### **8.4 Refereed Publications arising from this project**

- 1) McDonagh, C., Sheridan, F., Butler, T., MacCraith, B.D., "**Characterisation of sol-gel-derived silica films**", Journal of Non-Crystalline Solids Sept. 1995 (accepted for publication).
- 2) McDonagh, C., Sheridan, F., Butler, T., MacCraith, B.D., "**Characterisation of TEOS and Liquicoat derived sol-gel thin films**", Journal of Sol-Gel Science and Technology Sept. 1995 (accepted for publication).